

On the exact computation of linear frequency principle dynamics and its generalization*

Tao Luo

LUOTAO41@SJTU.EDU.CN

Zheng Ma

ZHENGMA@SJTU.EDU.CN

Zhi-Qin John Xu

XUZHIQIN@SJTU.EDU.CN

Yaoyu Zhang

ZHYY.SJTU@SJTU.EDU.CN

School of Mathematical Sciences, Institute of Natural Sciences, MOE-LSC and Qing Yuan Research Institute, Shanghai Jiao Tong University, Shanghai, 200240, P.R. China

Editor:

Abstract

Recent works show an intriguing phenomenon of Frequency Principle (F-Principle) that deep neural networks (DNNs) fit the target function from low to high frequency during the training, which provides insight into the training and generalization behavior of DNNs in complex tasks. In this paper, through analysis of an infinite-width two-layer NN in the neural tangent kernel (NTK) regime, we derive the exact differential equation, namely Linear Frequency-Principle (LFP) model, governing the evolution of NN output function in the frequency domain during the training. Our exact computation applies for general activation functions with no assumption on size and distribution of training data. This LFP model unravels that higher frequencies evolve polynomially or exponentially slower than lower frequencies depending on the smoothness/regularity of the activation function. We further bridge the gap between training dynamics and generalization by proving that LFP model implicitly minimizes a Frequency-Principle norm (FP-norm) of the learned function, by which higher frequencies are more severely penalized depending on the inverse of their evolution rate. Finally, we derive an *a priori* generalization error bound controlled by the FP-norm of the target function, which provides a theoretical justification for the empirical results that DNNs often generalize well for low frequency functions.

Keywords: two-layer neural network, neural tangent kernel, frequency principle, generalization, optimization

1. Introduction

Recently, an intriguing phenomenon of Frequency Principle (F-Principle) sheds light on understanding the success and failure of DNNs. It is discovered that, in various settings, deep neural networks (DNNs) fit the target function from low to high frequency during the training (Xu et al., 2019a; Rahaman et al., 2019; Xu et al., 2019b). The F-Principle implies that DNNs are biased toward a low-frequency fitting of the training data, which provides hints to the generalization of DNNs in practice (Xu et al., 2019b; Ma et al., 2020). The F-Principle provided valuable guidance in designing DNN-based algorithms (Cai et al., 2019; Biland et al., 2019; Jagtap et al., 2020; Liu et al., 2020). The convergence behavior from low to high frequency is also consistent with other empirical studies showing that DNNs

*. Authors are listed alphabetically.

increase the complexity of the output function during the training process quantified by various complexity measures (Arpit et al., 2017; Valle-Perez et al., 2019; Mingard et al., 2019; Nakkiran et al., 2019).

Despite of the rich practical implications of the F-Principle, the gap between F-Principle training dynamics and success or failure of DNNs (i.e., generalization performance) remains a key theoretical challenge. Bridging this gap requires an exact characterization of the F-Principle accounting for the conditions of overparameterization and finite training data in practice, which is not provided by existing theories (Basri et al., 2019; Bordelon et al., 2020; Cao et al., 2019; E et al., 2020)

In this work, based on mean-field analysis of an infinite-width two-layer NN in the NTK regime, we derive the exact differential equation, namely Linear Frequency-Principle (LFP) model, governing the evolution of NN output function in the frequency domain during the training. Our exact computation applies for general activation functions with no assumption on size and distribution of training data. Our LFP model rigorously characterizes the F-Principle and unravels that higher frequencies evolves polynomially or exponentially slower than lower frequencies depending on the smoothness/regularity of the activation function. We further prove that LFP dynamics implicitly minimizes a Frequency-Principle norm (FP-norm), by which higher frequencies are more severely penalized depending on the inverse of their evolution rate. Specifically, for 1-d regression problems, this optimization yields linear spline, cubic spline or their combination depending on parameter initialization for ReLU activation. Finally, we derive an *a priori* generalization error bound controlled by the FP-norm of the target function, which provides a unified qualitative explanation to the success and failure of DNNs. These three results are demonstrated by Theorems 1, 2 and 3, respectively. For a better understanding of how we arrive three theorems, we depict the sketch of proofs for each theorem in Fig. 1.

The structure of the paper is organized as follows. We review related works in Section 2. Before we present our results, we introduce some preliminaries in Section 3. Then, we show the exact computation of the LFP model in Section 4. In Section 5, we explicitize the implicit bias of the F-Principle by proving the equivalence between the LFP model and an optimization problem. Further, we estimate an *a priori* generalization error bound for the LFP model in Section 6. In Section 7, we use experiments to validate the effectiveness of the LFP model for ReLU and Tanh activation functions. Finally, we present conclusions and discussion in Section 8.

2. Related works

A series of works have devoted to reveal underlying mechanisms of the F-Principle. Xu (2018) and Xu et al. (2019b) show that the gradient of low-frequency loss exponentially dominates that of high-frequency ones when parameters are small for DNNs with tanh activation. A key mechanism of F-Principle has been pointed out that the low-frequency dominant gradient is a consequence of the smoothness of the activation function. Rahaman et al. (2019) later extend the framework of tanh activation function to the ReLU activation function. Luo et al. (2019) estimate the dynamics of different frequency components of the

Sketch of proofs for theorems

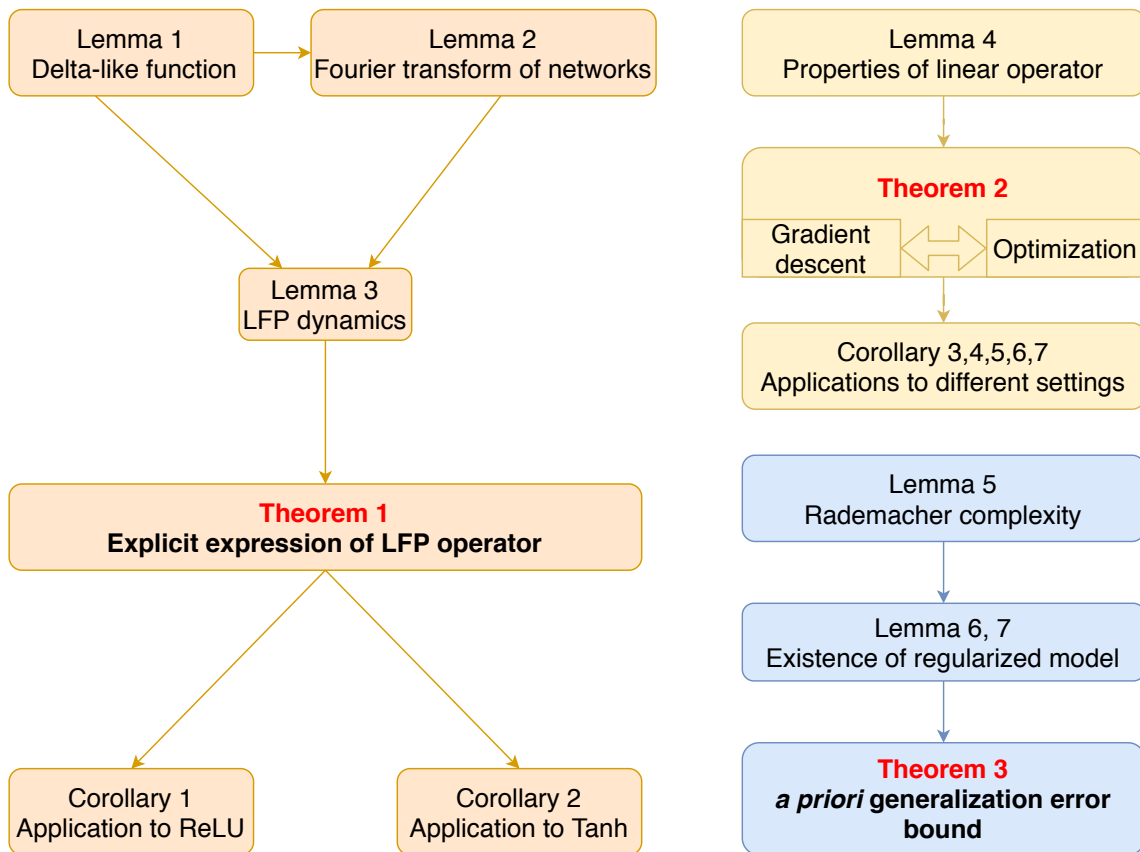


Figure 1: Main theoretical results and sketch of proofs.

loss function for arbitrary data distribution with mild regularity assumption and sufficient large size of training data size.

At the same time with our work, several parallel works also analyze the F-Principle (or spectral bias) in the NTK regime. Basri et al. (2019) and Cao et al. (2019) estimate the convergence speed of each frequency for two-layer wide ReLU networks in the NTK regime with the assumption of a sufficient large size of training data uniformly distributed on a hyper-sphere. Basri et al. (2020) release the assumption on data distribution to a nonuniform one, which is restricted to two-dimensional sphere, and they derive a similar frequency bias for two-layer wide ReLU networks in the NTK regime. Bordelon et al. (2020) study the dependence of the spectral bias on the sample size. Several other works also focus on studying the spectral of Gram matrix in the NTK regime (Arora et al., 2019; Yang and Salman, 2019).

In this work, our exact derivation of linear frequency principle dynamics makes no assumption about the distribution and size of training data. It is the first NN-derived quantitative model that not only shows the origin of the F-Principle but also can be used to analyze both its training and generalization consequence *.

3. Preliminaries

We provide some preliminary results in this section.

3.1 Fourier transforms

The Fourier transform of a function g is denoted by \hat{g} or $\mathcal{F}[g]$. The one-dimensional Fourier transform and its inverse transform is defined by

$$\mathcal{F}[g](\xi) = \mathcal{F}_{x \rightarrow \xi}[g](\xi) = \int_{\mathbb{R}} g(x) e^{-2\pi i \xi x} dx, \quad (1)$$

$$\mathcal{F}^{-1}[g](x) = \mathcal{F}_{\xi \rightarrow x}^{-1}[g](x) = \int_{\mathbb{R}} g(\xi) e^{2\pi i \xi x} d\xi. \quad (2)$$

Based on these, we define the high-dimensional Fourier transform and its inverse transform:

$$\mathcal{F}[g](\boldsymbol{\xi}) = \mathcal{F}_{\boldsymbol{x} \rightarrow \boldsymbol{\xi}}[g](\boldsymbol{\xi}) = \int_{\mathbb{R}^d} g(\boldsymbol{x}) e^{-2\pi i \boldsymbol{\xi} \cdot \boldsymbol{x}} d\boldsymbol{x}, \quad (3)$$

$$\mathcal{F}^{-1}[g](\boldsymbol{x}) = \mathcal{F}_{\boldsymbol{\xi} \rightarrow \boldsymbol{x}}^{-1}[g](\boldsymbol{x}) = \int_{\mathbb{R}^d} g(\boldsymbol{\xi}) e^{2\pi i \boldsymbol{\xi} \cdot \boldsymbol{x}} d\boldsymbol{\xi}. \quad (4)$$

Here and latter, the vector $\boldsymbol{x} \in \mathbb{R}^d$ and $\boldsymbol{x}^\perp = \boldsymbol{x} - (\boldsymbol{x} \cdot \hat{\boldsymbol{w}})\hat{\boldsymbol{w}}$ for a given $\boldsymbol{w} \in \mathbb{R}^d \setminus \{\mathbf{0}\}$ with $\hat{\boldsymbol{w}} = \boldsymbol{w}/\|\boldsymbol{w}\|$. We list some useful and well-known results for one-dimensional as well as high-dimensional Fourier transforms in Appendix A. To compute rigorously, we work in the theory of tempered distributions. Let $\mathcal{S}(\mathbb{R}^d)$ be the Schwartz space on \mathbb{R}^d and $\mathcal{S}'(\mathbb{R}^d) := (\mathcal{S}(\mathbb{R}^d))'$ is the space of tempered distributions. For any Schwartz function $\phi \in \mathcal{S}(\mathbb{R}^d)$ and any tempered distribution $\psi \in \mathcal{S}'(\mathbb{R}^d)$, we write the pairing $\langle \psi, \phi \rangle := \langle \psi, \phi \rangle_{\mathcal{S}'(\mathbb{R}^d), \mathcal{S}(\mathbb{R}^d)} = \psi(\phi)$, and then the Fourier transform of ψ is defined by

$$\langle \mathcal{F}[\psi], \phi \rangle = \langle \psi, \mathcal{F}[\phi] \rangle. \quad (5)$$

*. A previous incomplete version of this work is released at arXiv (Zhang et al., 2019).

3.2 High-dimensional delta-like function

Definition 1. Given a nonzero vector $\mathbf{w} \in \mathbb{R}^d$, we define the delta-like function $\delta_{\mathbf{w}} : \mathcal{S}(\mathbb{R}^d) \rightarrow \mathbb{R}$ such that for any $\phi \in \mathcal{S}(\mathbb{R}^d)$,

$$\langle \delta_{\mathbf{w}}, \phi \rangle = \int_{\mathbb{R}} \phi(y\mathbf{w}) \, dy. \quad (6)$$

Lemma 1 (Scaling property of delta-like function). Given any nonzero vector $\mathbf{w} \in \mathbb{R}^d$ with $\hat{\mathbf{w}} = \frac{\mathbf{w}}{\|\mathbf{w}\|}$, we have

$$\frac{1}{\|\mathbf{w}\|^d} \delta_{\hat{\mathbf{w}}} \left(\frac{\mathbf{x}}{\|\mathbf{w}\|} \right) = \delta_{\mathbf{w}}(\mathbf{x}). \quad (7)$$

Proof This is proved by changing of variables. In fact, for any $\phi \in \mathcal{S}(\mathbb{R}^d)$, we have

$$\begin{aligned} \left\langle \frac{1}{\|\mathbf{w}\|^d} \delta_{\hat{\mathbf{w}}} \left(\frac{\cdot}{\|\mathbf{w}\|} \right), \phi(\cdot) \right\rangle_{\mathcal{S}'(\mathbb{R}^d), \mathcal{S}(\mathbb{R}^d)} &= \langle \delta_{\hat{\mathbf{w}}}(\cdot), \phi(\|\mathbf{w}\|\cdot) \rangle_{\mathcal{S}'(\mathbb{R}^d), \mathcal{S}(\mathbb{R}^d)} \\ &= \int_{\mathbb{R}} \phi(\|\mathbf{w}\|y\hat{\mathbf{w}}) \, dy \\ &= \int_{\mathbb{R}} \phi(y\mathbf{w}) \, dy \\ &= \langle \delta_{\mathbf{w}}(\cdot), \phi(\cdot) \rangle_{\mathcal{S}'(\mathbb{R}^d), \mathcal{S}(\mathbb{R}^d)}. \end{aligned}$$

■

Lemma 2 (Fourier transforms of network functions). For any unit vector $\boldsymbol{\nu} \in \mathbb{R}^d$, any nonzero vector $\mathbf{w} \in \mathbb{R}^d$ with $\hat{\mathbf{w}} = \frac{\mathbf{w}}{\|\mathbf{w}\|}$, and $g \in \mathcal{S}'(\mathbb{R})$ with $\mathcal{F}[g] \in C(\mathbb{R})$, we have, in the sense of distribution,

$$(a) \quad \mathcal{F}_{\mathbf{x} \rightarrow \boldsymbol{\xi}}[g(\boldsymbol{\nu}^\top \mathbf{x})](\boldsymbol{\xi}) = \delta_{\boldsymbol{\nu}}(\boldsymbol{\xi}) \mathcal{F}[g](\boldsymbol{\xi}^\top \boldsymbol{\nu}), \quad (8)$$

$$(b) \quad \mathcal{F}_{\mathbf{x} \rightarrow \boldsymbol{\xi}}[g(\mathbf{w}^\top \mathbf{x} + b)](\boldsymbol{\xi}) = \delta_{\mathbf{w}}(\boldsymbol{\xi}) \mathcal{F}[g] \left(\frac{\boldsymbol{\xi}^\top \hat{\mathbf{w}}}{\|\mathbf{w}\|} \right) e^{2\pi i \frac{b}{\|\mathbf{w}\|} \boldsymbol{\xi}^\top \hat{\mathbf{w}}}, \quad (9)$$

$$(c) \quad \mathcal{F}_{\mathbf{x} \rightarrow \boldsymbol{\xi}}[\mathbf{x}g(\mathbf{w}^\top \mathbf{x} + b)](\boldsymbol{\xi}) = \frac{i}{2\pi} \nabla_{\boldsymbol{\xi}} \left[\delta_{\mathbf{w}}(\boldsymbol{\xi}) \mathcal{F}[g] \left(\frac{\boldsymbol{\xi}^\top \hat{\mathbf{w}}}{\|\mathbf{w}\|} \right) e^{2\pi i \frac{b}{\|\mathbf{w}\|} \boldsymbol{\xi}^\top \hat{\mathbf{w}}} \right]. \quad (10)$$

Proof Let $\phi \in \mathcal{S}(\mathbb{R}^d)$ be any test function.

(a) By direct calculation, we have

$$\begin{aligned} \langle \mathcal{F}_{\mathbf{x} \rightarrow \cdot} [g(\boldsymbol{\nu}^\top \mathbf{x})](\cdot), \phi(\cdot) \rangle_{\mathcal{S}'(\mathbb{R}^d), \mathcal{S}(\mathbb{R}^d)} &= \langle g(\boldsymbol{\nu}^\top \cdot), \mathcal{F}_{\mathbf{x} \rightarrow \cdot} [\phi(\mathbf{x})](\cdot) \rangle_{\mathcal{S}'(\mathbb{R}^d), \mathcal{S}(\mathbb{R}^d)} \\ &= \langle g(\cdot), \mathcal{F}_{y \rightarrow \cdot} [\phi(y\boldsymbol{\nu})](\cdot) \rangle_{\mathcal{S}'(\mathbb{R}), \mathcal{S}(\mathbb{R})} \\ &= \langle \mathcal{F}_{y \rightarrow \cdot} [g(y)](\cdot), \phi(\cdot \boldsymbol{\nu}) \rangle_{\mathcal{S}'(\mathbb{R}), \mathcal{S}(\mathbb{R})} \\ &= \langle \mathcal{F}[g](\cdot \boldsymbol{\nu}^\top \boldsymbol{\nu}), \phi(\cdot \boldsymbol{\nu}) \rangle_{\mathcal{S}'(\mathbb{R}), \mathcal{S}(\mathbb{R})} \\ &= \langle \delta_{\boldsymbol{\nu}}(\cdot) \mathcal{F}[g](\cdot^\top \boldsymbol{\nu}), \phi(\cdot) \rangle_{\mathcal{S}'(\mathbb{R}^d), \mathcal{S}(\mathbb{R}^d)}. \end{aligned}$$

(b) By part (a), we have in the distributional sense

$$\mathcal{F}_{\mathbf{x} \rightarrow \boldsymbol{\xi}}[g(\hat{\mathbf{w}}^\top \mathbf{x})](\boldsymbol{\xi}) = \delta_{\hat{\mathbf{w}}}(\boldsymbol{\xi}) \mathcal{F}[g](\boldsymbol{\xi}^\top \hat{\mathbf{w}}).$$

Note that

$$\mathcal{F}_{\mathbf{x} \rightarrow \boldsymbol{\xi}}[g(\mathbf{x} - \mathbf{x}_0)](\boldsymbol{\xi}) = \mathcal{F}_{\mathbf{x} \rightarrow \boldsymbol{\xi}}[g](\boldsymbol{\xi}) e^{-2\pi i \mathbf{x}_0^\top \boldsymbol{\xi}},$$

then

$$\begin{aligned} \mathcal{F}_{\mathbf{x} \rightarrow \boldsymbol{\xi}}[g(\hat{\mathbf{w}}^\top \mathbf{x} + b)](\boldsymbol{\xi}) &= \mathcal{F}_{\mathbf{x} \rightarrow \boldsymbol{\xi}}[g(\hat{\mathbf{w}}^\top (\mathbf{x} + b\hat{\mathbf{w}}))](\boldsymbol{\xi}) \\ &= \delta_{\hat{\mathbf{w}}}(\boldsymbol{\xi}) \mathcal{F}[g](\boldsymbol{\xi}^\top \hat{\mathbf{w}}) e^{2\pi i b \hat{\mathbf{w}}^\top \boldsymbol{\xi}}. \end{aligned}$$

Therefore

$$\begin{aligned} \mathcal{F}_{\mathbf{x} \rightarrow \boldsymbol{\xi}}[g(\mathbf{w}^\top \mathbf{x} + b)](\boldsymbol{\xi}) &= \mathcal{F}_{\mathbf{x} \rightarrow \boldsymbol{\xi}}[g(\hat{\mathbf{w}}^\top \|\mathbf{w}\| \mathbf{x} + b)](\boldsymbol{\xi}) \\ &= \frac{1}{\|\mathbf{w}\|^d} \mathcal{F}_{\mathbf{x} \rightarrow \boldsymbol{\xi}}[g(\hat{\mathbf{w}}^\top \mathbf{x} + b)] \left(\frac{\boldsymbol{\xi}}{\|\mathbf{w}\|} \right) \\ &= \frac{1}{\|\mathbf{w}\|^d} \delta_{\hat{\mathbf{w}}} \left(\frac{\boldsymbol{\xi}}{\|\mathbf{w}\|} \right) \mathcal{F}[g] \left(\frac{\boldsymbol{\xi}^\top \hat{\mathbf{w}}}{\|\mathbf{w}\|} \right) e^{2\pi i \frac{b}{\|\mathbf{w}\|} \hat{\mathbf{w}}^\top \boldsymbol{\xi}} \\ &= \delta_{\mathbf{w}}(\boldsymbol{\xi}) \mathcal{F}[g] \left(\frac{\boldsymbol{\xi}^\top \hat{\mathbf{w}}}{\|\mathbf{w}\|} \right) e^{2\pi i \frac{b}{\|\mathbf{w}\|} \hat{\mathbf{w}}^\top \boldsymbol{\xi}}. \end{aligned}$$

(c) This follows from part (b) and the fact that for any function $\tilde{g}(\mathbf{x})$

$$\mathcal{F}_{\mathbf{x} \rightarrow \boldsymbol{\xi}}[\mathbf{x} \tilde{g}(\mathbf{x})](\boldsymbol{\xi}) = \frac{i}{2\pi} \nabla_{\boldsymbol{\xi}} [\mathcal{F}[\tilde{g}](\boldsymbol{\xi})].$$

■

4. Exact derivation of LFP model

In this section, we first present the general form of the LFP model for two-layer neural networks. Then, we exactly compute the LFP model in the Fourier domain and derive the expressions for two commonly-used activation functions, i.e., $\text{ReLU}(x) := \max(x, 0)$ and $\tanh(x)$.

For any positive integer N , we denote the set $\{1, 2, \dots, N\}$ by $[N]$. The training dataset $S = \{(\mathbf{x}_i, y_i)\}_{i=1}^n$, where $\{\mathbf{x}_i\}_{i=1}^n$ are i.i.d. sampled from unknown distribution \mathcal{D} on a domain $\Omega \subset \mathbb{R}^d$ and $y_i = f(\mathbf{x}_i)$, $i \in [n]$ for some unknown function f .

4.1 Mean-field kernel dynamics in frequency domain

We suppose that $f \in C(\mathbb{R}^d) \cap L^2(\mathbb{R}^d)$ and that the activation function is locally H^1 and grows polynomially, i.e., $|\sigma(z)| \leq C|z|^p$ for some $p > 0$.

We consider the following gradient descent dynamics of the population risk R_S of a network function $f(\cdot, \boldsymbol{\theta})$ parameterized by $\boldsymbol{\theta}$

$$\begin{cases} \dot{\boldsymbol{\theta}} = -\nabla_{\boldsymbol{\theta}} R_S(\boldsymbol{\theta}), \\ \boldsymbol{\theta}(0) = \boldsymbol{\theta}_0, \end{cases} \quad (11)$$

where

$$R_S(\boldsymbol{\theta}) = \frac{1}{2} \sum_{i=1}^n (f(\mathbf{x}_i, \boldsymbol{\theta}) - y_i)^2. \quad (12)$$

Then the training dynamics of output function $f(\cdot, \boldsymbol{\theta})$ is

$$\begin{aligned} \frac{d}{dt} f(\mathbf{x}, \boldsymbol{\theta}) &= \nabla_{\boldsymbol{\theta}} f(\mathbf{x}, \boldsymbol{\theta}) \cdot \dot{\boldsymbol{\theta}} \\ &= -\nabla_{\boldsymbol{\theta}} f(\mathbf{x}, \boldsymbol{\theta}) \cdot \nabla_{\boldsymbol{\theta}} R_S(\boldsymbol{\theta}) \\ &= -\nabla_{\boldsymbol{\theta}} f(\mathbf{x}, \boldsymbol{\theta}) \cdot \sum_{i=1}^n \nabla_{\boldsymbol{\theta}} f(\mathbf{x}_i, \boldsymbol{\theta}) (f(\mathbf{x}_i, \boldsymbol{\theta}) - y_i) \\ &= -\sum_{i=1}^n K_m(\mathbf{x}, \mathbf{x}_i) (f(\mathbf{x}_i, \boldsymbol{\theta}) - y_i) \end{aligned}$$

where for time t the NTK evaluated at $(\mathbf{x}, \mathbf{x}') \in \Omega \times \Omega$ reads as

$$K_m(\mathbf{x}, \mathbf{x}') (t) = \nabla_{\boldsymbol{\theta}} f(\mathbf{x}, \boldsymbol{\theta}(t)) \cdot \nabla_{\boldsymbol{\theta}} f(\mathbf{x}', \boldsymbol{\theta}(t)). \quad (13)$$

The gradient descent of the linear model thus becomes

$$\frac{d}{dt} \left(f(\mathbf{x}, \boldsymbol{\theta}(t)) - f(\mathbf{x}) \right) = -\sum_{i=1}^n K_m(\mathbf{x}, \mathbf{x}_i) (t) \left(f(\mathbf{x}_i, \boldsymbol{\theta}(t)) - f(\mathbf{x}_i) \right). \quad (14)$$

Define the residual $\mathbf{u}(\mathbf{x}, t) = f(\mathbf{x}, \boldsymbol{\theta}(t)) - f(\mathbf{x})$ and the empirical density $\rho(\mathbf{x}) = \sum_{i=1}^n \delta(\mathbf{x} - \mathbf{x}_i)$. We further denote $u_\rho(\mathbf{x}) = \mathbf{u}(\mathbf{x}) \rho(\mathbf{x})$. Therefore the dynamics for u becomes

$$\frac{d}{dt} u(\mathbf{x}, t) = -\int_{\mathbb{R}^d} K_m(\mathbf{x}, \mathbf{x}') (t) u_\rho(\mathbf{x}', t) d\mathbf{x}'. \quad (15)$$

From now on, we consider the two-layer neural network

$$f(\mathbf{x}, \boldsymbol{\theta}) = \frac{1}{\sqrt{m}} \sum_{j=1}^m a_j \sigma(\mathbf{w}_j^\top \mathbf{x} + b_j) \quad (16)$$

$$= \frac{1}{\sqrt{m}} \sum_{j=1}^m \sigma^*(\mathbf{x}, \mathbf{q}_j). \quad (17)$$

where the vector of all parameters $\boldsymbol{\theta} = \text{vec}(\{\mathbf{q}_j\}_{j=1}^m)$ is formed of the parameters for each neuron $\mathbf{q}_j = (a_j, \mathbf{w}_j^\top, b_j)^\top \in \mathbb{R}^{d+2}$ and $\sigma^*(\mathbf{x}, \mathbf{q}_j) = a_j \sigma(\mathbf{w}_j^\top \mathbf{x} + b_j)$ for $j \in [m]$. We consider the kernel regime that $m \gg 1$ and assume that $b \sim \mathcal{N}(0, \sigma_b^2)$ with $\sigma_b \gg 1$. For the two-layer network, its NTK can be calculated as follows

$$K_m(\mathbf{x}, \mathbf{x}') (t) = \frac{1}{m} \sum_{j=1}^m \nabla_{\mathbf{q}_j} \sigma^*(\mathbf{x}, \mathbf{q}_j(t)) \cdot \sigma^*(\mathbf{x}', \mathbf{q}_j(t)), \quad (18)$$

where the parameters \mathbf{q}_j 's are evaluated at time t . Under some weak condition and for sufficiently large m , E et al. e20 (2020) proved that the dynamics (15), with a high probability, converges to the following dynamics for any $t \in \mathbb{R}$

$$\frac{d}{dt}u(\mathbf{x}, t) = - \int_{\mathbb{R}^d} K(\mathbf{x}, \mathbf{x}')u_\rho(\mathbf{x}', t) d\mathbf{x}'. \quad (19)$$

where the kernel only depends on the initial distribution of parameters and reads as

$$K(\mathbf{x}, \mathbf{x}') = \mathbb{E}_{\mathbf{q}} \nabla_{\mathbf{q}} \sigma^*(\mathbf{x}, \mathbf{q}) \cdot \sigma^*(\mathbf{x}', \mathbf{q}) \quad (20)$$

$$\begin{aligned} &= \mathbb{E}_{\mathbf{q}} (\sigma(\mathbf{w}^\top \mathbf{x} + b) \sigma(\mathbf{w}^\top \mathbf{x}' + b) + a^2 \sigma'(\mathbf{w}^\top \mathbf{x} + b) \sigma'(\mathbf{w}^\top \mathbf{x}' + b) \mathbf{x}^\top \mathbf{x}' \\ &\quad + a^2 \sigma'(\mathbf{w}^\top \mathbf{x} + b) \sigma'(\mathbf{w}^\top \mathbf{x}' + b)). \end{aligned} \quad (21)$$

Intuitively, this is because $K_m(\mathbf{x}, \mathbf{x}') (t) = K(\mathbf{x}, \mathbf{x}') + O(\frac{1}{\sqrt{m}})$ according to the law of large numbers. In the following, we analyze (19) and calculate its formulation in the frequency domain.

We start with the following lemma.

Lemma 3 (LFP dynamics for general DNNs). *The dynamics (19) has the following expression in the frequency domain*

$$\langle \partial_t \mathcal{F}[u], \phi \rangle = \langle \mathcal{L}[\mathcal{F}[u_\rho]], \phi \rangle, \quad (22)$$

where $\mathcal{L}[\cdot]$ is called *Linear F-Principle (LFP) operator* is given by

$$\mathcal{L}[\mathcal{F}[u_\rho]] = - \int_{\mathbb{R}^d} \hat{K}(\boldsymbol{\xi}, \boldsymbol{\xi}') \mathcal{F}[u_\rho](\boldsymbol{\xi}') d\boldsymbol{\xi}',$$

and

$$\hat{K}(\boldsymbol{\xi}, \boldsymbol{\xi}') := \mathbb{E}_{\mathbf{q}} \hat{K}_{\mathbf{q}}(\boldsymbol{\xi}, \boldsymbol{\xi}') := \mathbb{E}_{\mathbf{q}} \mathcal{F}_{\mathbf{x} \rightarrow \boldsymbol{\xi}}[\nabla_{\mathbf{q}} \sigma^*(\mathbf{x}, \mathbf{q})] \cdot \overline{\mathcal{F}_{\mathbf{x}' \rightarrow \boldsymbol{\xi}'}[\nabla_{\mathbf{q}} \sigma^*(\mathbf{x}', \mathbf{q})]}. \quad (23)$$

The expectation $\mathbb{E}_{\mathbf{q}}$ is taken w.r.t. initial distribution of parameters.

Proof

For any $\phi \in \mathcal{S}(\mathbb{R}^d)$. since $\partial_t u$ is in $\mathcal{S}'(\mathbb{R}^d)$ and locally integrable, we have

$$\begin{aligned} \langle \partial_t \mathcal{F}[u], \phi \rangle &= \langle \partial_t u, \mathcal{F}[\phi] \rangle \\ &= \int_{\mathbb{R}^d} \partial_t u(\mathbf{x}, t) \int_{\mathbb{R}^d} \phi(\boldsymbol{\xi}) e^{-i2\pi \mathbf{x} \cdot \boldsymbol{\xi}} d\boldsymbol{\xi} d\mathbf{x} \\ &= - \int_{\mathbb{R}^d} \int_{\mathbb{R}^d} K(\mathbf{x}, \mathbf{x}') u_\rho(\mathbf{x}') d\mathbf{x}' \int_{\mathbb{R}^d} \phi(\boldsymbol{\xi}) e^{-i2\pi \mathbf{x} \cdot \boldsymbol{\xi}} d\boldsymbol{\xi} d\mathbf{x} \\ &= - \int_{\mathbb{R}^{3d}} K(\mathbf{x}, \mathbf{x}') u_\rho(\mathbf{x}') d\mathbf{x}' \phi(\boldsymbol{\xi}) e^{-i2\pi \mathbf{x} \cdot \boldsymbol{\xi}} d\boldsymbol{\xi} d\mathbf{x} \\ &= - \int_{\mathbb{R}^{3d}} \mathbb{E}_{\mathbf{q}} \nabla_{\mathbf{q}} \sigma^*(\mathbf{x}, \mathbf{q}) \cdot \nabla_{\mathbf{q}} \sigma^*(\mathbf{x}', \mathbf{q}) u_\rho(\mathbf{x}') d\mathbf{x}' \phi(\boldsymbol{\xi}) e^{-i2\pi \mathbf{x} \cdot \boldsymbol{\xi}} d\boldsymbol{\xi} d\mathbf{x} \\ &= - \mathbb{E}_{\mathbf{q}} \int_{\mathbb{R}^d} \nabla_{\mathbf{q}} \sigma^*(\mathbf{x}', \mathbf{q}) u_\rho(\mathbf{x}') d\mathbf{x}' \cdot \int_{\mathbb{R}^{2d}} \nabla_{\mathbf{q}} \sigma^*(\mathbf{x}, \mathbf{q}) e^{-i2\pi \mathbf{x} \cdot \boldsymbol{\xi}} \phi(\boldsymbol{\xi}) d\boldsymbol{\xi} d\mathbf{x} \\ &= - \mathbb{E}_{\mathbf{q}} \int_{\mathbb{R}^d} \nabla_{\mathbf{q}} \sigma^*(\mathbf{x}', \mathbf{q}) u_\rho(\mathbf{x}') d\mathbf{x}' \cdot \langle \mathcal{F}_{\mathbf{x} \rightarrow \cdot}[\nabla_{\mathbf{q}} \sigma^*(\mathbf{x}, \mathbf{q})](\cdot), \phi(\cdot) \rangle. \end{aligned}$$

Since

$$\int_{\mathbb{R}^d} \nabla_{\mathbf{q}} \sigma^*(\mathbf{x}', \mathbf{q}) u_\rho(\mathbf{x}') d\mathbf{x}' = \int_{\mathbb{R}^d} \overline{\mathcal{F}_{\mathbf{x}' \rightarrow \xi'}[\nabla_{\mathbf{q}} \sigma^*(\mathbf{x}', \mathbf{q})](\xi')} \mathcal{F}_{\mathbf{x}' \rightarrow \xi'}[u_\rho](\xi') d\xi',$$

we have

$$\begin{aligned} \langle \partial_t \mathcal{F}[u], \phi \rangle &= -\mathbb{E}_{\mathbf{q}} \int_{\mathbb{R}^d} \overline{\mathcal{F}_{\mathbf{x}' \rightarrow \xi'}[\nabla_{\mathbf{q}} \sigma^*(\mathbf{x}', \mathbf{q})](\xi')} \mathcal{F}_{\mathbf{x}' \rightarrow \xi'}[u_\rho](\xi') d\xi' \cdot \langle \mathcal{F}_{\mathbf{x} \rightarrow \cdot}[\nabla_{\mathbf{q}} \sigma^*(\mathbf{x}, \mathbf{q})](\cdot), \phi(\cdot) \rangle \\ &= -\mathbb{E}_{\mathbf{q}} \int_{\mathbb{R}^{2d}} \overline{\mathcal{F}_{\mathbf{x}' \rightarrow \xi'}[\nabla_{\mathbf{q}} \sigma^*(\mathbf{x}', \mathbf{q})](\xi')} \cdot \mathcal{F}_{\mathbf{x} \rightarrow \xi}[\nabla_{\mathbf{q}} \sigma^*(\mathbf{x}, \mathbf{q})](\xi) \mathcal{F}_{\mathbf{x}' \rightarrow \xi'}[u_\rho](\xi') d\xi' \phi(\xi) d\xi \\ &= -\int_{\mathbb{R}^{2d}} \hat{K}(\xi, \xi') \mathcal{F}[u_\rho](\xi') d\xi' \phi(\xi) d\xi \\ &= \langle \mathcal{L}[\mathcal{F}[u_\rho]], \phi \rangle. \end{aligned}$$

■

4.2 LFP dynamics derived for two-layer networks

In this section, we derive the LFP dynamics for two-layer networks with general activation function. The key difficulty comes from the repeated integral representation of the operator. By using the Laplace method in a proper way, we overcome this difficulty and arrive at a simpler expression for the dynamics.

To simplified the notation, we define $\mathbf{g}_1(z) := (\sigma(z), a\sigma'(z))^\top$ and $\mathbf{g}_2(z) := a\sigma'(z)$ for $z \in \mathbb{R}$. Then

$$\mathbf{g}_1(\mathbf{w}^\top \mathbf{x} + b) = \begin{pmatrix} \sigma(\mathbf{w}^\top \mathbf{x} + b) \\ a\sigma'(\mathbf{w}^\top \mathbf{x} + b) \end{pmatrix} = \begin{pmatrix} \partial_a [a\sigma(\mathbf{w}^\top \mathbf{x} + b)] \\ \partial_b [a\sigma(\mathbf{w}^\top \mathbf{x} + b)] \end{pmatrix}, \quad (24)$$

$$\mathbf{g}_2(\mathbf{w}^\top \mathbf{x} + b)\mathbf{x} = \nabla_{\mathbf{w}} [a\sigma(\mathbf{w}^\top \mathbf{x} + b)] = a\sigma'(\mathbf{w}^\top \mathbf{x} + b)\mathbf{x}. \quad (25)$$

The following theorem is the key to the exact expression of LFP dynamics for two-layer networks.

Assumption 1. *We assume that the initial distribution of $\mathbf{q} = (a, \mathbf{w}^\top, b)^\top$ satisfies the following conditions:*

- (i) *independence of a, \mathbf{w}, b : $\rho_{\mathbf{q}}(\mathbf{q}) = \rho_a(a)\rho_{\mathbf{w}}(\mathbf{w})\rho_b(b)$.*
- (ii) *zero-mean and finite variance of b : $\mathbb{E}_b b = 0$ and $\mathbb{E}_b b^2 = \sigma_b^2 < \infty$.*
- (iii) *radially symmetry of \mathbf{w} : $\rho_{\mathbf{w}}(\mathbf{w}) = \rho_{\mathbf{w}}(\|\mathbf{w}\|\mathbf{e}_1)$ where $\mathbf{e}_1 = (1, 0, \dots, 0)^\top$.*

Theorem 1 (Main result: explicit expression of LFP operator for two-layer networks). *Suppose that Assumption 1 holds. If $\sigma_b \gg 1$, then the dynamics (19) has the following expression,*

$$\langle \partial_t \mathcal{F}[u], \phi \rangle = -\langle \mathcal{L}[\mathcal{F}[u_\rho]], \phi \rangle + O(\sigma_b^{-3}), \quad (26)$$

where $\phi \in \mathcal{S}(\mathbb{R}^d)$ is a test function and the LFP operator is given by

$$\begin{aligned} \mathcal{L}[\mathcal{F}[u_\rho]] &= \frac{\Gamma(d/2)}{2\sqrt{2}\pi^{(d+1)/2}\sigma_b\|\boldsymbol{\xi}\|^{d-1}} \mathbb{E}_{a,r} \left[\frac{1}{r} \mathcal{F}[g_1] \left(\frac{\|\boldsymbol{\xi}\|}{r} \right) \cdot \mathcal{F}[g_1] \left(\frac{-\|\boldsymbol{\xi}\|}{r} \right) \right] \mathcal{F}[u_\rho](\boldsymbol{\xi}) \\ &\quad - \frac{\Gamma(d/2)}{2\sqrt{2}\pi^{(d+1)/2}\sigma_b} \nabla \cdot \left(\mathbb{E}_{a,r} \left[\frac{1}{r\|\boldsymbol{\xi}\|^{d-1}} \mathcal{F}[g_2] \left(\frac{\|\boldsymbol{\xi}\|}{r} \right) \mathcal{F}[g_2] \left(-\frac{\|\boldsymbol{\xi}\|}{r} \right) \right] \nabla \mathcal{F}[u_\rho](\boldsymbol{\xi}) \right). \end{aligned} \quad (27)$$

The expectations are taken w.r.t. initial parameter distribution. Here $r = \|\mathbf{w}\|$ with the probability density $\rho_r(r) := \frac{2\pi^{d/2}}{\Gamma(d/2)} \rho_{\mathbf{w}}(r\mathbf{e}_1)r^{d-1}$, $\mathbf{e}_1 = (1, 0, \dots, 0)^\top$.

Remark 1. The operator \mathcal{L} presents a unified framework for general activation functions.

Remark 2. The derivatives of most activation functions decay in the Fourier domain, e.g., ReLU, tanh, and sigmoid. Hence, the dynamics in (26) for higher frequency component is slower, i.e., *F-Principle*.

Remark 3. The last term in Eq. (27) arises from the evolution of \mathbf{w} is much more complicated, without which our experiments show that the LFP model can still predict the learning results of two-layer wide NNs.

Proof For simplicity, we assume that $b \sim \mathcal{N}(0, \sigma_b^2)$, $\sigma_b \gg 1$ in this proof. It is straightforward to extend the proof to general distributions for b as long as it is zero-mean and with variance $\sigma_b \gg 1$.

1. Divide into two parts. Note that

$$\begin{pmatrix} g_1(\mathbf{w}^\top \mathbf{x} + b) \\ \mathbf{x} g_2(\mathbf{w}^\top \mathbf{x} + b) \end{pmatrix} = \begin{pmatrix} \partial_a [a\sigma(\mathbf{w}^\top \mathbf{x} + b)] \\ \partial_b [a\sigma(\mathbf{w}^\top \mathbf{x} + b)] \\ \nabla_{\mathbf{w}} [a\sigma(\mathbf{w}^\top \mathbf{x} + b)] \end{pmatrix} = \nabla_{\mathbf{q}} \sigma^*(\mathbf{x}, \mathbf{q}). \quad (28)$$

One can split the Fourier transformed kernel \hat{K} into two parts, more precisely,

$$\hat{K} = \mathbb{E}_{\mathbf{q}} \hat{K}_{\mathbf{q}}, \quad \hat{K}_{\mathbf{q}} = \hat{K}_{a,b} + \hat{K}_{\mathbf{w}},$$

where

$$\begin{aligned} \hat{K}_{\mathbf{q}}(\boldsymbol{\xi}, \boldsymbol{\xi}') &= \mathbb{E}_{\mathbf{q}} \mathcal{F}_{\mathbf{x} \rightarrow \boldsymbol{\xi}} [\nabla_{\mathbf{q}} \sigma^*(\mathbf{x}, \mathbf{q})] \cdot \overline{\mathcal{F}_{\mathbf{x}' \rightarrow \boldsymbol{\xi}'} [\nabla_{\mathbf{q}} \sigma^*(\mathbf{x}', \mathbf{q})]}, \\ \hat{K}_{a,b}(\boldsymbol{\xi}, \boldsymbol{\xi}') &= \mathcal{F}[g_1(\mathbf{w}^\top \mathbf{x} + b)] \cdot \overline{\mathcal{F}[g_1(\mathbf{w}^\top \mathbf{x}' + b)]}, \\ \hat{K}_{\mathbf{w}}(\boldsymbol{\xi}, \boldsymbol{\xi}') &= \mathcal{F}[\mathbf{x} g_2(\mathbf{w}^\top \mathbf{x} + b)] \cdot \overline{\mathcal{F}[\mathbf{x} g_2(\mathbf{w}^\top \mathbf{x}' + b)]}. \end{aligned}$$

For any $\phi, \psi \in \mathcal{S}(\mathbb{R}^d)$, we have

$$\langle \hat{K}_{\mathbf{q}}, \phi \otimes \psi \rangle := \langle \hat{K}_{\mathbf{q}}, \phi \otimes \psi \rangle_{\mathcal{S}'(\mathbb{R}^{2d}), \mathcal{S}(\mathbb{R}^{2d})} = \int_{\mathbb{R}^{2d}} \hat{K}_{\mathbf{q}}(\boldsymbol{\xi}, \boldsymbol{\xi}') \phi(\boldsymbol{\xi}) \psi(\boldsymbol{\xi}') \, d\boldsymbol{\xi} \, d\boldsymbol{\xi}'. \quad (29)$$

The expressions for $\hat{K}_{a,b}$ and $\hat{K}_{\mathbf{w}}$ are similar.

2. Calculate $\hat{K}_{a,b}(\boldsymbol{\xi}, \boldsymbol{\xi}')$. Since

$$\hat{K}_{a,b}(\boldsymbol{\xi}, \boldsymbol{\xi}') = \delta_{\mathbf{w}}(\boldsymbol{\xi}) \delta_{\mathbf{w}}(\boldsymbol{\xi}') \mathcal{F}[g_1] \left(\frac{\boldsymbol{\xi}^\top \hat{\mathbf{w}}}{\|\mathbf{w}\|} \right) \cdot \overline{\mathcal{F}[g_1] \left(\frac{\boldsymbol{\xi}'^\top \hat{\mathbf{w}}}{\|\mathbf{w}\|} \right)} e^{2\pi i b (\boldsymbol{\xi} - \boldsymbol{\xi}')^\top \hat{\mathbf{w}} / \|\mathbf{w}\|},$$

we have

$$\begin{aligned}\langle \hat{K}_{a,b}, \phi \otimes \psi \rangle &= \int_{\mathbb{R}^{2d}} \delta_{\mathbf{w}}(\boldsymbol{\xi}) \delta_{\mathbf{w}}(\boldsymbol{\xi}') \mathcal{F}[\mathbf{g}_1] \left(\frac{\boldsymbol{\xi}^\top \hat{\mathbf{w}}}{\|\mathbf{w}\|} \right) \cdot \overline{\mathcal{F}[\mathbf{g}_1] \left(\frac{\boldsymbol{\xi}'^\top \hat{\mathbf{w}}}{\|\mathbf{w}\|} \right)} e^{2\pi i b (\boldsymbol{\xi} - \boldsymbol{\xi}')^\top \hat{\mathbf{w}} / \|\mathbf{w}\|} \phi(\boldsymbol{\xi}) \psi(\boldsymbol{\xi}') \, d\boldsymbol{\xi} \, d\boldsymbol{\xi}' \\ &= \int_{\mathbb{R} \times \mathbb{R}} \phi(\eta \mathbf{w}) \psi(\eta' \mathbf{w}) \mathcal{F}[\mathbf{g}_1](\eta) \cdot \overline{\mathcal{F}[\mathbf{g}_1](\eta')} e^{2\pi i b (\eta - \eta')} \, d\eta \, d\eta'.\end{aligned}$$

By assumption $b \sim \mathcal{N}(0, \sigma_b^2)$, i.e., $\rho_b(b) = \frac{1}{\sqrt{2\pi}\sigma_b} e^{-\frac{b^2}{2\sigma_b^2}}$, then $\mathcal{F}[\rho_b](\eta) = e^{-2\pi^2\sigma_b^2\eta^2}$.

$$\begin{aligned}\mathbb{E}_b \left(e^{2\pi i b (\eta - \eta')} \right) &= \int_{\mathbb{R}} \frac{1}{\sqrt{2\pi}\sigma_b} e^{-b^2/2\sigma_b^2} e^{2\pi i b (\eta - \eta')} \, db \\ &= \mathcal{F}[\rho_b](-(\eta - \eta')) \\ &= e^{-2\pi^2\sigma_b^2(\eta - \eta')^2}.\end{aligned}$$

Therefore

$$\begin{aligned}\mathbb{E}_b \left[\langle \hat{K}_{a,b}, \phi \otimes \psi \rangle \right] &= \int_{\mathbb{R} \times \mathbb{R}} \phi(\eta \mathbf{w}) \psi(\eta' \mathbf{w}) \mathcal{F}[\mathbf{g}_1](\eta) \cdot \overline{\mathcal{F}[\mathbf{g}_1](\eta')} \mathbb{E}_b \left[e^{2\pi i b (\eta - \eta')} \right] \, d\eta \, d\eta' \\ &= \int_{\mathbb{R} \times \mathbb{R}} \phi(\eta \mathbf{w}) \psi(\eta' \mathbf{w}) \mathcal{F}[\mathbf{g}_1](\eta) \cdot \overline{\mathcal{F}[\mathbf{g}_1](\eta')} e^{-2\pi^2\sigma_b^2(\eta - \eta')^2} \, d\eta \, d\eta'.\end{aligned}$$

Applying the Laplace method, we have

$$\begin{aligned}\mathbb{E}_b \left[\langle \hat{K}_{a,b}, \phi \otimes \psi \rangle \right] &= \int_{\mathbb{R}} \phi(\eta \mathbf{w}) \mathcal{F}[\mathbf{g}_1](\eta) \cdot \left[\int_{\mathbb{R}} \psi(\eta' \mathbf{w}) \overline{\mathcal{F}[\mathbf{g}_1](\eta')} e^{-2\pi^2\sigma_b^2(\eta - \eta')^2} \, d\eta' \right] \, d\eta \\ &= \int_{\mathbb{R}} \phi(\eta \mathbf{w}) \mathcal{F}[\mathbf{g}_1](\eta) \cdot \left[\psi(\eta \mathbf{w}) \overline{\mathcal{F}[\mathbf{g}_1](\eta)} \frac{1}{\sqrt{2\pi}\sigma_b} + O(\sigma_b^{-3}) \right] \, d\eta \\ &= \frac{1}{\sqrt{2\pi}\sigma_b} \int_{\mathbb{R}} \phi(\eta \mathbf{w}) \psi(\eta \mathbf{w}) \mathcal{F}[\mathbf{g}_1](\eta) \cdot \overline{\mathcal{F}[\mathbf{g}_1](\eta)} \, d\eta + O(\sigma_b^{-3}).\end{aligned}$$

Next we consider the expectation with respect to \mathbf{w} . Up to error of order $O(\sigma_c^{-3})$, we have

$$\begin{aligned}\mathbb{E}_{\mathbf{w}, b} \left[\langle \hat{K}_{a,b}, \phi \otimes \psi \rangle \right] &= \mathbb{E}_{\mathbf{w}} \left[\frac{1}{\sqrt{2\pi}\sigma_b} \int_{\mathbb{R}} \phi(\eta \mathbf{w}) \psi(\eta \mathbf{w}) \mathcal{F}[\mathbf{g}_1](\eta) \cdot \overline{\mathcal{F}[\mathbf{g}_1](\eta)} \, d\eta \right] \\ &= \int_{\mathbb{R}^{d+1}} \frac{1}{\sqrt{2\pi}\sigma_b} \phi(\eta \mathbf{w}) \psi(\eta \mathbf{w}) \mathcal{F}[\mathbf{g}_1](\eta) \cdot \overline{\mathcal{F}[\mathbf{g}_1](\eta)} \rho_{\mathbf{w}}(\mathbf{w}) \, d\mathbf{w} \, d\eta.\end{aligned}$$

Here we assume that $\rho_{\mathbf{w}}$ is radially symmetric so $\rho_{\mathbf{w}}(\mathbf{w})$ is a function of $r := \|\mathbf{w}\|$ only. By using spherical coordinate system, we have

$$\begin{aligned}1 &= \int_{\mathbb{R}^d} \rho_{\mathbf{w}}(\mathbf{w}) \, d\mathbf{w} \\ &= \int_{\mathbb{R}^d} \rho_{\mathbf{w}}(\|\mathbf{w}\| \mathbf{e}_1) \, d\mathbf{w} \\ &= \int_{\mathbb{R}^+} \int_{\mathbb{S}^{d-1}} \rho_{\mathbf{w}}(r \mathbf{e}_1) r^{d-1} \, d\hat{\mathbf{w}} \, dr \\ &= \int_{\mathbb{R}^+} \rho_r(r) \, dr,\end{aligned}$$

where $\hat{\mathbf{w}} \in \mathbb{S}^{d-1}$ and we define

$$\rho_r(r) := \int_{\mathbb{S}^{d-1}} \rho_{\mathbf{w}}(r\mathbf{e}_1) r^{d-1} d\hat{\mathbf{w}} = \frac{2\pi^{d/2}}{\Gamma(d/2)} \rho_{\mathbf{w}}(r\mathbf{e}_1) r^{d-1}, \quad (30)$$

where $\Gamma(\cdot)$ is the gamma function. Then we introduce the following change of variables,

$$\begin{cases} \zeta = \eta\mathbf{w}, \\ r = \|\mathbf{w}\|, \end{cases}$$

whose the Jacobian determinant is

$$\det \left(\frac{\partial(\zeta, r)}{\partial(\mathbf{w}, \eta)} \right) = \det \begin{bmatrix} \eta & 0 & \cdots & 0 & w_1 \\ 0 & \eta & \cdots & 0 & w_2 \\ \vdots & \vdots & \ddots & \vdots & \vdots \\ 0 & 0 & \cdots & \eta & w_d \\ w_1/r & w_2/r & \cdots & w_d/r & 0 \end{bmatrix} = -r\eta^{d-1} = -r \left(\frac{\|\zeta\|}{r} \right)^{d-1}.$$

Thus

$$\begin{cases} \mathbf{w} = \frac{r\zeta}{\|\zeta\|} \\ \eta = \frac{\|\zeta\|}{r}, \end{cases} \quad (31)$$

and its Jacobian determinant is

$$\det \left(\frac{\partial(\mathbf{w}, \eta)}{\partial(\zeta, r)} \right) = -\frac{r^{d-1}}{r\|\zeta\|^{d-1}}.$$

So one can obtain,

$$\begin{aligned} \mathbb{E}_{\mathbf{w}, b} \left[\langle \hat{K}_{a,b}, \phi \otimes \psi \rangle \right] &= \int_{\mathbb{R}^{d+1}} \frac{1}{\sqrt{2\pi}\sigma_b} \phi(\eta\mathbf{w}) \psi(\eta\mathbf{w}) \mathcal{F}[\mathbf{g}_1](\eta) \cdot \overline{\mathcal{F}[\mathbf{g}_1](\eta)} \rho_{\mathbf{w}}(r\mathbf{e}_1) d\mathbf{w} d\eta \\ &= \int_{\mathbb{R}^d \times \mathbb{R}^+} \frac{1}{\sqrt{2\pi}\sigma_b} \phi(\zeta) \psi(\zeta) \mathcal{F}[\mathbf{g}_1] \left(\frac{\|\zeta\|}{r} \right) \cdot \overline{\mathcal{F}[\mathbf{g}_1] \left(\frac{\|\zeta\|}{r} \right)} \frac{r^{d-1}}{r\|\zeta\|^{d-1}} \rho_{\mathbf{w}}(r\mathbf{e}_1) d\zeta dr \\ &= \int_{\mathbb{R}^d \times \mathbb{R}^+} \frac{1}{\sqrt{2\pi}\sigma_b} \phi(\zeta) \psi(\zeta) \mathcal{F}[\mathbf{g}_1] \left(\frac{\|\zeta\|}{r} \right) \cdot \overline{\mathcal{F}[\mathbf{g}_1] \left(\frac{\|\zeta\|}{r} \right)} \frac{1}{r\|\zeta\|^{d-1}} \left[\frac{\Gamma(d/2)}{2\pi^{d/2}} \rho_r(r) \right] d\zeta dr \\ &= \frac{\Gamma(d/2)}{2\sqrt{2\pi}^{(d+1)/2}\sigma_b} \int_{\mathbb{R}^d} \phi(\zeta) \int_{\mathbb{R}^+} \left[\frac{1}{r\|\zeta\|^{d-1}} \mathcal{F}[\mathbf{g}_1] \left(\frac{\|\zeta\|}{r} \right) \cdot \overline{\mathcal{F}[\mathbf{g}_1] \left(\frac{\|\zeta\|}{r} \right)} \right] \psi(\zeta) \rho_r(r) dr d\zeta, \end{aligned}$$

Therefore taking $\psi = \mathcal{F}[u_\rho]$, we have

$$\begin{aligned} \mathcal{L}_{a,b}[\mathcal{F}[u_\rho]] &= \frac{\Gamma(d/2)}{2\sqrt{2\pi}^{(d+1)/2}\sigma_b \|\xi\|^{d-1}} \mathbb{E}_{a,r} \left[\frac{1}{r} \mathcal{F}[\mathbf{g}_1] \left(\frac{\|\xi\|}{r} \right) \cdot \overline{\mathcal{F}[\mathbf{g}_1] \left(\frac{\|\xi\|}{r} \right)} \right] \mathcal{F}[u_\rho](\xi) \\ &= \frac{\Gamma(d/2)}{2\sqrt{2\pi}^{(d+1)/2}\sigma_b \|\xi\|^{d-1}} \mathbb{E}_{a,r} \left[\frac{1}{r} \mathcal{F}[\mathbf{g}_1] \left(\frac{\|\xi\|}{r} \right) \cdot \mathcal{F}[\mathbf{g}_1] \left(-\frac{\|\xi\|}{r} \right) \right] \mathcal{F}[u_\rho](\xi). \quad (32) \end{aligned}$$

3. Calculate $\hat{K}_{\mathbf{w}}(\boldsymbol{\xi}, \boldsymbol{\xi}')$. Since

$$\hat{K}_{\mathbf{w}}(\boldsymbol{\xi}, \boldsymbol{\xi}') = \frac{1}{4\pi^2} \nabla_{\boldsymbol{\xi}} \left[\delta_{\mathbf{w}}(\boldsymbol{\xi}) \mathcal{F}[g_2] \left(\frac{\boldsymbol{\xi}^\top \hat{\mathbf{w}}}{\|\mathbf{w}\|} \right) e^{2\pi i b \boldsymbol{\xi}^\top \hat{\mathbf{w}} / \|\mathbf{w}\|} \right] \cdot \nabla_{\boldsymbol{\xi}'} \left[\overline{\delta_{\mathbf{w}}(\boldsymbol{\xi}') \mathcal{F}[g_2] \left(\frac{\boldsymbol{\xi}'^\top \hat{\mathbf{w}}}{\|\mathbf{w}\|} \right) e^{-2\pi i b \boldsymbol{\xi}'^\top \hat{\mathbf{w}} / \|\mathbf{w}\|}} \right],$$

we have

$$\begin{aligned} & \langle \hat{K}_{\mathbf{w}}, \phi \otimes \psi \rangle \\ &= \frac{1}{4\pi^2} \int_{\mathbb{R}^d} \phi(\boldsymbol{\xi}) \nabla_{\boldsymbol{\xi}} \left[\delta_{\mathbf{w}}(\boldsymbol{\xi}) \mathcal{F}[g_2] \left(\frac{\boldsymbol{\xi}^\top \hat{\mathbf{w}}}{\|\mathbf{w}\|} \right) e^{2\pi i b \boldsymbol{\xi}^\top \hat{\mathbf{w}} / \|\mathbf{w}\|} \right] d\boldsymbol{\xi} \\ & \quad \cdot \int_{\mathbb{R}^d} \psi(\boldsymbol{\xi}') \nabla_{\boldsymbol{\xi}'} \left[\overline{\delta_{\mathbf{w}}(\boldsymbol{\xi}') \mathcal{F}[g_2] \left(\frac{\boldsymbol{\xi}'^\top \hat{\mathbf{w}}}{\|\mathbf{w}\|} \right) e^{-2\pi i b \boldsymbol{\xi}'^\top \hat{\mathbf{w}} / \|\mathbf{w}\|}} \right] d\boldsymbol{\xi}' \\ &= \frac{1}{4\pi^2} \int_{\mathbb{R}^d} \nabla_{\boldsymbol{\xi}} \phi(\boldsymbol{\xi}) \delta_{\mathbf{w}}(\boldsymbol{\xi}) \mathcal{F}[g_2] \left(\frac{\boldsymbol{\xi}^\top \hat{\mathbf{w}}}{\|\mathbf{w}\|} \right) e^{2\pi i b \boldsymbol{\xi}^\top \hat{\mathbf{w}} / \|\mathbf{w}\|} d\boldsymbol{\xi} \\ & \quad \cdot \int_{\mathbb{R}^d} \nabla_{\boldsymbol{\xi}'} \psi(\boldsymbol{\xi}') \overline{\delta_{\mathbf{w}}(\boldsymbol{\xi}') \mathcal{F}[g_2] \left(\frac{\boldsymbol{\xi}'^\top \hat{\mathbf{w}}}{\|\mathbf{w}\|} \right) e^{-2\pi i b \boldsymbol{\xi}'^\top \hat{\mathbf{w}} / \|\mathbf{w}\|}} d\boldsymbol{\xi}' \\ &= \int_{\mathbb{R} \times \mathbb{R}} \nabla \phi(\eta \mathbf{w}) \cdot \nabla \psi(\eta' \mathbf{w}) \mathcal{F}[g_2](\eta) \cdot \overline{\mathcal{F}[g_2](\eta')} e^{2\pi i b(\eta - \eta')} d\eta d\eta'. \end{aligned}$$

By the same computation as for $\hat{K}_{a,b}(\boldsymbol{\xi}, \boldsymbol{\xi}')$, we can get

$$\begin{aligned} & \mathbb{E}_{\mathbf{w},b} \left[\langle \hat{K}_{\mathbf{w}}, \phi \otimes \psi \rangle \right] \\ &= \frac{\Gamma(d/2)}{2\sqrt{2}\pi^{(d+1)/2}\sigma_b} \int_{\mathbb{R}^d} \nabla \phi(\boldsymbol{\zeta}) \cdot \int_{\mathbb{R}^+} \left[\frac{1}{r\|\boldsymbol{\zeta}\|^{d-1}} \mathcal{F}[g_2] \left(\frac{\|\boldsymbol{\zeta}\|}{r} \right) \cdot \overline{\mathcal{F}[g_2] \left(\frac{\|\boldsymbol{\zeta}\|}{r} \right)} \right] \nabla \psi(\boldsymbol{\zeta}) \rho_r(r) dr d\boldsymbol{\zeta} \\ &= \frac{\Gamma(d/2)}{2\sqrt{2}\pi^{(d+1)/2}\sigma_b} \int_{\mathbb{R}^d} \nabla \phi(\boldsymbol{\zeta}) \cdot \mathbb{E}_{a,r} \left[\frac{1}{r\|\boldsymbol{\zeta}\|^{d-1}} \mathcal{F}[g_2] \left(\frac{\|\boldsymbol{\zeta}\|}{r} \right) \cdot \overline{\mathcal{F}[g_2] \left(\frac{\|\boldsymbol{\zeta}\|}{r} \right)} \right] \nabla \psi(\boldsymbol{\zeta}) d\boldsymbol{\zeta} \\ &= -\frac{\Gamma(d/2)}{2\sqrt{2}\pi^{(d+1)/2}\sigma_b} \int_{\mathbb{R}^d} \phi(\boldsymbol{\zeta}) \nabla \cdot \left\{ \mathbb{E}_{a,r} \left[\frac{1}{r\|\boldsymbol{\zeta}\|^{d-1}} \mathcal{F}[g_2] \left(\frac{\|\boldsymbol{\zeta}\|}{r} \right) \cdot \overline{\mathcal{F}[g_2] \left(\frac{\|\boldsymbol{\zeta}\|}{r} \right)} \right] \nabla \psi(\boldsymbol{\zeta}) \right\} d\boldsymbol{\zeta}. \end{aligned}$$

Thus taking $\psi(\boldsymbol{\xi}) = \mathcal{F}[u_\rho](\boldsymbol{\xi})$, we have

$$\mathcal{L}_{\mathbf{w}}[\mathcal{F}[u_\rho](\boldsymbol{\xi})] = -\frac{\Gamma(d/2)}{2\sqrt{2}\pi^{(d+1)/2}\sigma_b} \nabla \cdot \left(\mathbb{E}_{a,r} \left[\frac{1}{r\|\boldsymbol{\xi}\|^{d-1}} \mathcal{F}[g_2] \left(\frac{\|\boldsymbol{\xi}\|}{r} \right) \mathcal{F}[g_2] \left(-\frac{\|\boldsymbol{\xi}\|}{r} \right) \right] \nabla \mathcal{F}[u_\rho](\boldsymbol{\xi}) \right). \quad (33)$$

Finally, one can plug (32) and (33) into (22) and obtain the dynamics (26). \blacksquare

4.3 Exact LFP model for common activation functions

Based on (27), we derive the exact LFP dynamics for the cases where the activation function is ReLU and tanh.

Corollary 1 (LFP operator for ReLU activation function). *Suppose that Assumption 1 holds. If $\sigma_b \gg 1$ and $\sigma = \text{ReLU}$, then the dynamics (19) has the following expression,*

$$\langle \partial_t \mathcal{F}[u], \phi \rangle = -\langle \mathcal{L}[\mathcal{F}[u_\rho]], \phi \rangle + O(\sigma_b^{-3}), \quad (34)$$

where $\phi \in \mathcal{S}(\mathbb{R}^d)$ is a test function and the LFP operator reads as

$$\begin{aligned} \mathcal{L}[\mathcal{F}[u_\rho]] &= \frac{\Gamma(d/2)}{2\sqrt{2}\pi^{(d+1)/2}\sigma_b} \mathbb{E}_{a,r} \left[\frac{r^3}{16\pi^4 \|\boldsymbol{\xi}\|^{d+3}} + \frac{a^2 r}{4\pi^2 \|\boldsymbol{\xi}\|^{d+1}} \right] \mathcal{F}[u_\rho](\boldsymbol{\xi}) \\ &\quad - \frac{\Gamma(d/2)}{2\sqrt{2}\pi^{(d+1)/2}\sigma_b} \nabla \cdot \left(\mathbb{E}_{a,r} \left[\frac{a^2 r}{4\pi^2 \|\boldsymbol{\xi}\|^{d+1}} \right] \nabla \mathcal{F}[u_\rho](\boldsymbol{\xi}) \right). \end{aligned} \quad (35)$$

The expectations are taken w.r.t. initial parameter distribution. Here $r = \|\mathbf{w}\|$ with the probability density $\rho_r(r) := \frac{2\pi^{d/2}}{\Gamma(d/2)} \rho_{\mathbf{w}}(r\mathbf{e}_1) r^{d-1}$, $\mathbf{e}_1 = (1, 0, \dots, 0)^\top$.

Proof Let

$$f_a(\mathbf{x}) := \nabla_a [a \text{ReLU}(\mathbf{w} \cdot \mathbf{x} + b)] = \text{ReLU}(\mathbf{w} \cdot \mathbf{x} + b), \quad (36)$$

$$g_a(z) := \text{ReLU}(z), \quad (37)$$

$$f_b(\mathbf{x}) := \nabla_b [a \text{ReLU}(\mathbf{w} \cdot \mathbf{x} + b)] = aH(\mathbf{w} \cdot \mathbf{x} + b), \quad (38)$$

$$g_b(z) := aH(z), \quad (39)$$

so $\mathbf{g}_1(z) = (g_a(z), g_b(z))^\top$ and $g_2(z) = g_b(z)$. Then

$$\mathcal{F}[g_a](\xi) = -\frac{1}{4\pi^2 \xi^2} + \frac{i}{4\pi} \delta'(\xi), \quad (40)$$

$$\mathcal{F}[g_b](\xi) = a \left[\frac{1}{i2\pi\xi} + \frac{1}{2} \delta(\xi) \right], \quad (41)$$

By ignoring all $\delta(\xi)$ and $\delta'(\xi)$ related to only the trivial $\mathbf{0}$ -frequency, we obtain

$$\frac{1}{r} \mathcal{F}[g_a] \left(\frac{\|\boldsymbol{\xi}\|}{r} \right) \mathcal{F}[g_a] \left(\frac{-\|\boldsymbol{\xi}\|}{r} \right) = \frac{r^3}{16\pi^4 \|\boldsymbol{\xi}\|^4}, \quad (42)$$

$$\frac{1}{r} \mathcal{F}[g_b] \left(\frac{\|\boldsymbol{\xi}\|}{r} \right) \mathcal{F}[g_b] \left(\frac{-\|\boldsymbol{\xi}\|}{r} \right) = \frac{a^2 r}{4\pi^2 \|\boldsymbol{\xi}\|^2}. \quad (43)$$

We then obtain (35) by plugging these into (27). ■

Corollary 2 (LFP operator for tanh activation function). *Suppose that Assumption 1 holds. If $\sigma_b \gg 1$ and $\sigma = \text{tanh}$, then the dynamics (19) has the following expression,*

$$\langle \partial_t \mathcal{F}[u], \phi \rangle = -\langle \mathcal{L}[\mathcal{F}[u_\rho]], \phi \rangle + O(\sigma_b^{-3}), \quad (44)$$

where $\phi \in \mathcal{S}(\mathbb{R}^d)$ is a test function and the LFP operator reads as

$$\begin{aligned} \mathcal{L}[\mathcal{F}[u_\rho]] &= \frac{\Gamma(d/2)}{2\sqrt{2}\pi^{(d+1)/2}\sigma_b \|\boldsymbol{\xi}\|^{d-1}} \mathbb{E}_{a,r} \left[\frac{\pi^2}{r} \text{csch}^2 \left(\frac{\pi^2 \|\boldsymbol{\xi}\|}{r} \right) + \frac{4\pi^4 a^2 \|\boldsymbol{\xi}\|^2}{r^3} \text{csch}^2 \left(\frac{\pi^2 \|\boldsymbol{\xi}\|}{r} \right) \right] \mathcal{F}[u_\rho](\boldsymbol{\xi}) \\ &\quad - \frac{\Gamma(d/2)}{2\sqrt{2}\pi^{(d+1)/2}\sigma_b} \nabla \cdot \left(\mathbb{E}_{a,r} \left[\frac{4\pi^4 a^2}{r^3 \|\boldsymbol{\xi}\|^{d-3}} \text{csch}^2 \left(\frac{\pi^2 \|\boldsymbol{\xi}\|}{r} \right) \right] \nabla \mathcal{F}[u_\rho](\boldsymbol{\xi}) \right). \end{aligned} \quad (45)$$

The expectations are taken w.r.t. initial parameter distribution. Here $r = \|\mathbf{w}\|$ with the probability density $\rho_r(r) := \frac{2\pi^{d/2}}{\Gamma(d/2)}\rho_{\mathbf{w}}(r\mathbf{e}_1)r^{d-1}$, $\mathbf{e}_1 = (1, 0, \dots, 0)^\top$.

Proof Let

$$f_a(\mathbf{x}) := \nabla_a [a \tanh(\mathbf{w} \cdot \mathbf{x} + b)] = \tanh(\mathbf{w} \cdot \mathbf{x} + b), \quad (46)$$

$$g_a(z) := \tanh(z), \quad (47)$$

$$f_b(\mathbf{x}) := \nabla_b [a \tanh(\mathbf{w} \cdot \mathbf{x} + b)] = a \operatorname{sech}^2(\mathbf{w} \cdot \mathbf{x} + b), \quad (48)$$

$$g_b(z) := a \operatorname{sech}^2(z), \quad (49)$$

so $\mathbf{g}_1(z) = (g_a(z), g_b(z))^\top$ and $g_2(z) = g_b(z)$. Then

$$\mathcal{F}[g_a](\xi) = -i\pi \operatorname{csch}(\pi^2 \xi), \quad (50)$$

$$\mathcal{F}[g_b](\xi) = 2\pi^2 a \xi \operatorname{csch}(\pi^2 \xi). \quad (51)$$

By ignoring all $\delta(\xi)$ and $\delta'(\xi)$ related to only the trivial $\mathbf{0}$ -frequency, we obtain

$$\frac{1}{r} \mathcal{F}[g_a] \left(\frac{\|\boldsymbol{\xi}\|}{r} \right) \mathcal{F}[g_a] \left(\frac{-\|\boldsymbol{\xi}\|}{r} \right) = \frac{\pi^2}{r} \operatorname{csch}^2 \left(\frac{\pi^2 \|\boldsymbol{\xi}\|}{r} \right), \quad (52)$$

$$\frac{1}{r} \mathcal{F}[g_b] \left(\frac{\|\boldsymbol{\xi}\|}{r} \right) \mathcal{F}[g_b] \left(\frac{-\|\boldsymbol{\xi}\|}{r} \right) = \frac{4\pi^4 a^2 \|\boldsymbol{\xi}\|^2}{r^3} \operatorname{csch}^2 \left(\frac{\pi^2 \|\boldsymbol{\xi}\|}{r} \right). \quad (53)$$

We then obtain (45) by plugging these into (27). ■

5. Explicitizing the implicit bias of the F-Principle

In the following sections, we analyze a simplified LFP model with ReLU activation function in (35) as follows,

$$\partial_t \mathcal{F}[u] = \mathbb{E}_{a,r} \left[\frac{r^3}{16\pi^4 \|\boldsymbol{\xi}\|^{d+3}} + \frac{a^2 r}{4\pi^2 \|\boldsymbol{\xi}\|^{d+1}} \right] \mathcal{F}[u_\rho](\boldsymbol{\xi}). \quad (54)$$

We discard the last term in Eq. (35) arising from the evolution of \mathbf{w} . The reasons are two folds. First, experiments show that Eq. (54) is accurately enough to predict the wide two-layer NN output after training. Second, the last term in Eq. (35) is too complicated to analyze for now.

In the LFP model, the solution is implicitly regularized by a decaying coefficient for different frequencies of $\mathcal{F}[u]$ throughout the training. For a quantitative analysis of this solution, we explicitize such an implicit dynamical regularization by a constrained optimization problem as follows.

5.1 An equivalent optimization problem to the gradient flow dynamics

First, we present a general theorem that the long-time limit solution of a gradient flow dynamics is equivalent to the solution of a constrained optimization problem.

Let H_1 and H_2 be two separable Hilbert spaces and $\mathcal{P} : H_1 \rightarrow H_2$ is a bounded linear operator. Let $\mathcal{P}^* : H_2 \rightarrow H_1$ be the adjoint operator of \mathcal{P} , defined by

$$\langle \mathcal{P}\phi_1, \phi_2 \rangle_{H_2} = \langle \phi_1, \mathcal{P}^*\phi_2 \rangle_{H_1}, \quad \text{for all } \phi_1 \in H_1, \phi_2 \in H_2. \quad (55)$$

Lemma 4. *Suppose that H_1 and H_2 are two separable Hilbert spaces and $\mathcal{P} : H_1 \rightarrow H_2$ and $\mathcal{P}^* : H_2 \rightarrow H_1$ is the adjoint of \mathcal{P} . Then all eigenvalues of $\mathcal{P}^*\mathcal{P}$ and $\mathcal{P}\mathcal{P}^*$ are non-negative. Moreover, they have the same positive spectrum. If in particular, we assume that the operator $\mathcal{P}\mathcal{P}^*$ is surjective, then the operator $\mathcal{P}^*\mathcal{P}$ is invertible.*

Proof We consider the eigenvalue problem $\mathcal{P}^*\mathcal{P}\phi_1 = \lambda\phi_1$. Taking inner product with ϕ_1 , we have $\langle \phi_1, \mathcal{P}^*\mathcal{P}\phi_1 \rangle_{H_1} = \lambda\|\phi_1\|_{H_1}^2$. Note that the left hand side is $\|\mathcal{P}\phi_1\|_{H_2}^2$ which is non-negative. Thus $\lambda \geq 0$. Similarly, the eigenvalues of $\mathcal{P}\mathcal{P}^*$ are also non-negative.

Now if $\mathcal{P}^*\mathcal{P}$ has a positive eigenvalue $\lambda > 0$, then $\mathcal{P}^*\mathcal{P}\phi_1 = \lambda\phi_1$ with non-zero vector $\phi_1 \in H_1$. It follows that $\mathcal{P}\mathcal{P}^*(\mathcal{P}\phi_1) = \lambda(\mathcal{P}\phi_1)$. It is sufficient to prove that $\mathcal{P}\phi_1$ is non-zero. Indeed, if $\mathcal{P}\phi_1 = 0$, then $\mathcal{P}^*\mathcal{P}\phi_1 = 0$ and $\lambda = 0$ which contradicts with our assumption. Therefore, any positive eigenvalue of $\mathcal{P}^*\mathcal{P}$ is an eigenvalue of $\mathcal{P}\mathcal{P}^*$. Similarly, any positive eigenvalue of $\mathcal{P}\mathcal{P}^*$ is an eigenvalue of $\mathcal{P}^*\mathcal{P}$.

Next, suppose that $\mathcal{P}\mathcal{P}^*$ is surjective. We show that $\mathcal{P}\mathcal{P}^*\phi_2 = 0$ has only the trivial solution $\phi_2 = 0$. In fact, $\mathcal{P}\mathcal{P}^*\phi_2 = 0$ implies that $\|\mathcal{P}^*\phi_2\|_{H_1}^2 = \langle \phi_2, \mathcal{P}\mathcal{P}^*\phi_2 \rangle_{H_2} = 0$, i.e., $\mathcal{P}^*\phi_2 = 0$. Thanks to the surjectivity of $\mathcal{P}\mathcal{P}^*$, there exists a vector $\phi_3 \in H_2$ such that $\phi_2 = \mathcal{P}\mathcal{P}^*\phi_3$. Let $\phi_1 = \mathcal{P}^*\phi_3 \in H_1$. Hence $\phi_2 = \mathcal{P}\phi_1$ and $\mathcal{P}^*\mathcal{P}\phi_1 = 0$. Taking inner product with ϕ_1 , we have $\|\mathcal{P}\phi_1\|_{H_2}^2 = \langle \phi_1, \mathcal{P}^*\mathcal{P}\phi_1 \rangle_{H_1} = 0$, i.e., $\phi_2 = \mathcal{P}\phi_1 = 0$. Therefore $\mathcal{P}\mathcal{P}^*$ is injective. This with the surjectivity assumption of $\mathcal{P}\mathcal{P}^*$ leads to that $\mathcal{P}\mathcal{P}^*$ is invertible. ■

Remark 4. *For the finite dimensional case $H_2 = \mathbb{R}^n$, conditions for the operator \mathcal{P} in Lemma 4 are reduced to that the matrix \mathbf{P} has rank n (full rank).*

Given $g \in H_2$, we consider the following two problems.

(i) The initial value problem

$$\begin{cases} \frac{d\phi}{dt} &= \mathcal{P}^*(g - \mathcal{P}\phi) \\ \phi(0) &= \phi_{\text{ini}}. \end{cases}$$

Since this equation is linear and with nonpositive eigenvalues on the right hand side, there exists a unique global-in-time solution $\phi(t)$ for all $t \in [0, +\infty)$ satisfying the initial condition. Moreover, the long-time limit $\lim_{t \rightarrow +\infty} \phi(t)$ exists and will be denoted as ϕ_∞ .

(ii) The minimization problem

$$\begin{aligned} &\min_{\phi - \phi_{\text{ini}} \in H_1} \|\phi - \phi_{\text{ini}}\|_{H_1}, \\ &\text{s.t. } \mathcal{P}\phi = g. \end{aligned}$$

In the following, we will show it has a unique minimizer which is denoted as h_{min} .

Now we show the following equivalent theorem.

Theorem 2 (Equivalence between gradient descent and optimization problems). *Suppose that $\mathcal{P}\mathcal{P}^*$ is surjective. The above Problems (i) and (ii) are equivalent in the sense that $\phi_\infty = \phi_{\min}$. More precisely, we have*

$$\phi_\infty = h_{\min} = \mathcal{P}^*(\mathcal{P}\mathcal{P}^*)^{-1}(g - \mathcal{P}\phi_{\text{ini}}) + \phi_{\text{ini}}. \quad (56)$$

Proof Let $\tilde{\phi} = \phi - \phi_{\text{ini}}$ and $\tilde{g} = g - \mathcal{P}\phi_{\text{ini}}$. Then it is sufficient to show the following problems (i') and (ii') are equivalent.

(i') The initial value problem

$$\begin{cases} \frac{d\tilde{\phi}}{dt} = \mathcal{P}^*(\tilde{g} - \mathcal{P}\tilde{\phi}) \\ \tilde{\phi}(0) = 0. \end{cases}$$

(ii') The minimization problem

$$\begin{aligned} & \min_{\tilde{\phi}} \|\tilde{\phi}\|_{H_1}^2, \\ & \text{s.t. } \mathcal{P}\tilde{\phi} = \tilde{g}. \end{aligned}$$

We claim that $\tilde{\phi}_{\min} = \mathcal{P}^*(\mathcal{P}\mathcal{P}^*)^{-1}\tilde{g}$. Thanks to Lemma 4, $\mathcal{P}\mathcal{P}^*$ is invertible, and thus ϕ_{\min} is well-defined and satisfies that $\mathcal{P}\phi_{\min} = \tilde{g}$. It remains to show that this solution is unique. In fact, for any $\tilde{\phi}$ satisfying $\mathcal{P}\tilde{\phi} = \tilde{g}$, we have

$$\begin{aligned} \langle \tilde{\phi} - \tilde{\phi}_{\min}, \tilde{\phi}_{\min} \rangle_{H_1} &= \langle \tilde{\phi} - \tilde{\phi}_{\min}, \mathcal{P}^*(\mathcal{P}\mathcal{P}^*)^{-1}\tilde{g} \rangle_{H_1} \\ &= \langle \mathcal{P}(\tilde{\phi} - \tilde{\phi}_{\min}), (\mathcal{P}\mathcal{P}^*)^{-1}\tilde{g} \rangle_{H_2} \\ &= \langle \mathcal{P}\tilde{\phi}, (\mathcal{P}\mathcal{P}^*)^{-1}\tilde{g} \rangle_{H_2} - \langle \mathcal{P}\tilde{\phi}_{\min}, (\mathcal{P}\mathcal{P}^*)^{-1}\tilde{g} \rangle_{H_2} \\ &= 0. \end{aligned}$$

Therefore,

$$\|\tilde{\phi}\|_{H_1}^2 = \|\tilde{\phi}_{\min}\|_{H_1}^2 + \|\tilde{\phi} - \tilde{\phi}_{\min}\|_{H_1}^2 \geq \|\tilde{\phi}_{\min}\|_{H_1}^2.$$

The equality holds if and only if $\tilde{\phi} = \tilde{\phi}_{\min}$.

For problem (i'), from the theory of ordinary differential equations on Hilbert spaces, we have that its solution can be written as

$$\tilde{\phi}(t) = \mathcal{P}^*(\mathcal{P}\mathcal{P}^*)^{-1}\tilde{g} + \sum_{i \in \mathcal{I}} c_i v_i \exp(-\lambda_i t),$$

where λ_i , $i \in \mathcal{I}$ are positive eigenvalues of $\mathcal{P}\mathcal{P}^*$, \mathcal{I} is an index set with at most countable cardinality, and v_i , $i \in \mathcal{I}$ are eigenvectors in H_1 . Thus $\tilde{\phi}_\infty = \tilde{\phi}_{\min} = \mathcal{P}^*(\mathcal{P}\mathcal{P}^*)^{-1}\tilde{g}$.

Finally, by back substitution, we have

$$\phi_\infty = \phi_{\min} = \mathcal{P}^*(\mathcal{P}\mathcal{P}^*)^{-1}\tilde{g} + \phi_0 = \mathcal{P}^*(\mathcal{P}\mathcal{P}^*)^{-1}(g - \mathcal{P}\phi_{\text{ini}}) + \phi_{\text{ini}}. \quad \blacksquare$$

The following corollaries are obtained directly from Theorem 2.

Corollary 3. Let ϕ be the parameter vector θ in $H_1 = \mathbb{R}^m$, g be the outputs of the training data \mathbf{Y} , and \mathbf{P} be a full rank matrix in the linear DNN model. Then the following two problems are equivalent in the sense that $\theta_\infty = \theta_{\min}$.

(A1) The initial value problem

$$\begin{cases} \frac{d\theta}{dt} = \mathbf{P}^*(\mathbf{Y} - \mathbf{P}\theta) \\ \theta(0) = \theta_{\text{ini}}. \end{cases}$$

(A2) The minimization problem

$$\begin{aligned} & \min_{\theta - \theta_{\text{ini}} \in \mathbb{R}^m} \|\theta - \theta_{\text{ini}}\|_2, \\ & \text{s.t. } \mathbf{P}\theta = \mathbf{Y}. \end{aligned}$$

The next corollary is a weighted version of Theorem 2.

Corollary 4. Let H_1 and H_2 be two separable Hilbert spaces and $\Gamma : H_1 \rightarrow H_1$ be an injective operator. Define the Hilbert space $H_\Gamma := \text{Im}(\Gamma)$. Let $g \in H_2$ and $\mathcal{P} : H_\Gamma \rightarrow H_2$ be an operator such that $\mathcal{P}\mathcal{P}^* : H_2 \rightarrow H_2$ is surjective. Then $\Gamma^{-1} : H_\Gamma \rightarrow H_1$ exists and H_Γ is a Hilbert space with norm $\|\phi\|_{H_\Gamma} := \|\Gamma^{-1}\phi\|_{H_1}$. Moreover, the following two problems are equivalent in the sense that $\phi_\infty = \phi_{\min}$.

(B1) The initial value problem

$$\begin{cases} \frac{d\phi}{dt} = \Gamma\Gamma^*\mathcal{P}^*(g - \mathcal{P}\phi) \\ \phi(0) = \phi_{\text{ini}}. \end{cases}$$

(B2) The minimization problem

$$\begin{aligned} & \min_{\phi - \phi_{\text{ini}} \in H_\Gamma} \|\phi - \phi_{\text{ini}}\|_{H_\Gamma}, \\ & \text{s.t. } \mathcal{P}\phi = g. \end{aligned}$$

Proof The operator $\Gamma : H_1 \rightarrow H_\Gamma$ is bijective. Hence $\Gamma^{-1} : H_\Gamma \rightarrow H_1$ is well-defined and H_Γ with norm $\|\cdot\|_{H_\Gamma}$ is a Hilbert space. The equivalence result holds by applying Theorem 2 with proper replacements. More precisely, we replace ϕ by $\Gamma^{-1}\phi$ and \mathcal{P} by $\mathcal{P}\Gamma$. \blacksquare

Corollary 5. Let $\gamma : \mathbb{R}^d \rightarrow \mathbb{R}^+$ be a positive function, h be a function in $L^2(\mathbb{R}^d)$ and $\phi = \mathcal{F}[h]$. The operator $\Gamma : L^2(\mathbb{R}^d) \rightarrow L^2(\mathbb{R}^d)$ is defined by $[\Gamma\phi](\xi) = \gamma(\xi)\phi(\xi)$, $\xi \in \mathbb{R}^d$. Define the Hilbert space $H_\Gamma := \text{Im}(\Gamma)$. Let $\mathbf{X} = (\mathbf{x}_1, \dots, \mathbf{x}_n)^\top \in \mathbb{R}^{n \times d}$, $\mathbf{Y} = (y_1, \dots, y_n)^\top \in \mathbb{R}^n$ and $\mathcal{P} : H_\Gamma \rightarrow \mathbb{R}^n$ be a surjective operator

$$\mathcal{P} : \phi \mapsto \left(\int_{\mathbb{R}^d} \phi(\xi) e^{2\pi i \mathbf{x}_1^\top \xi} d\xi, \dots, \int_{\mathbb{R}^d} \phi(\xi) e^{2\pi i \mathbf{x}_n^\top \xi} d\xi \right)^\top = (h(\mathbf{x}_1), \dots, h(\mathbf{x}_n))^\top. \quad (57)$$

Then the following two problems are equivalent in the sense that $\phi_\infty = \phi_{\min}$.

(C1) The initial value problem

$$\begin{cases} \frac{d\phi(\boldsymbol{\xi})}{dt} = (\gamma(\boldsymbol{\xi}))^2 \sum_{i=1}^n \left(y_i e^{-2\pi i \mathbf{x}_i^\top \boldsymbol{\xi}} - [\phi * e^{-2\pi i \mathbf{x}_i^\top (\cdot)}](\boldsymbol{\xi}) \right) \\ \phi(0) = \phi_{\text{ini}}. \end{cases}$$

(C2) The minimization problem

$$\begin{aligned} \min_{\phi - \phi_{\text{ini}} \in H_\Gamma} \int_{\mathbb{R}^d} (\gamma(\boldsymbol{\xi}))^{-2} |\phi(\boldsymbol{\xi}) - \phi_{\text{ini}}(\boldsymbol{\xi})|^2 d\boldsymbol{\xi}, \\ \text{s.t. } h(\mathbf{x}_i) = y_i, \quad i = 1, \dots, n. \end{aligned}$$

Proof Let $H_1 = L^2(\mathbb{R}^d)$, $H_2 = \mathbb{R}^n$, $g = \mathbf{Y}$. By definition, Γ is injective. Then by Corollary 4, we have that $\Gamma^{-1} : H_\Gamma \rightarrow L^2(\mathbb{R}^d)$ exists and H_Γ is a Hilbert space with norm $\|\phi\|_{H_\Gamma} := \|\Gamma^{-1}\phi\|_{L^2(\mathbb{R}^d)}$. Moreover, $\|\phi - \phi_{\text{ini}}\|_{H_\Gamma}^2 = \int_{\mathbb{R}^d} (\gamma(\boldsymbol{\xi}))^{-2} |\phi(\boldsymbol{\xi}) - \phi_{\text{ini}}(\boldsymbol{\xi})|^2 d\boldsymbol{\xi}$. We note that $[\mathcal{P}^* \mathbf{Y}](\boldsymbol{\xi}) = \sum_{i=1}^n y_i e^{-2\pi i \mathbf{x}_i^\top \boldsymbol{\xi}}$ for all $\boldsymbol{\xi} \in \mathbb{R}^d$. Thus

$$\begin{aligned} [\mathcal{P}^* \mathcal{P}\phi](\boldsymbol{\xi}) &= \left[\mathcal{P}^* \left(\int_{\mathbb{R}^d} \phi(\boldsymbol{\xi}') e^{2\pi i \mathbf{x}_i^\top \boldsymbol{\xi}'} d\boldsymbol{\xi}' \right)_{i=1}^n \right](\boldsymbol{\xi}) \\ &= \sum_{i=1}^n \int_{\mathbb{R}^d} \phi(\boldsymbol{\xi}') e^{2\pi i \mathbf{x}_i^\top \boldsymbol{\xi}'} d\boldsymbol{\xi}' e^{-2\pi i \mathbf{x}_i^\top \boldsymbol{\xi}} \\ &= \sum_{i=1}^n \int_{\mathbb{R}^d} \phi(\boldsymbol{\xi}') e^{-2\pi i \mathbf{x}_i^\top (\boldsymbol{\xi} - \boldsymbol{\xi}')} d\boldsymbol{\xi}' \\ &= \sum_{i=1}^n \left[\phi * e^{-2\pi i \mathbf{x}_i^\top (\cdot)} \right](\boldsymbol{\xi}). \end{aligned}$$

The equivalence result then follows from Corollary 4. ■

We remark that $\mathcal{P}^* \mathcal{P}\phi = \sum_{i=1}^n \mathcal{F}[h\delta_{\mathbf{x}_i}]$, where $\delta_{\mathbf{x}_i}(\cdot) = \delta(\cdot - \mathbf{x}_i)$, $i = 1, \dots, n$. Therefore problem (C1) can also be written as:

$$\begin{cases} \frac{d\mathcal{F}[h]}{dt} = \gamma^2 \sum_{i=1}^n (y_i \mathcal{F}[\delta_{\mathbf{x}_i}] - \mathcal{F}[h\delta_{\mathbf{x}_i}]) \\ \mathcal{F}[h](\mathbf{0}) = \mathcal{F}[h]_{\text{ini}}. \end{cases}$$

In the following, we study the discretized version of this dynamics-optimization problem (C1&C2).

Corollary 6. Let $\gamma : \mathbb{Z}^d \rightarrow \mathbb{R}^+$ be a positive function defined on lattice \mathbb{Z}^d and $\phi = \mathcal{F}[h]$. The operator $\Gamma : \ell^2(\mathbb{Z}^d) \rightarrow \ell^2(\mathbb{Z}^d)$ is defined by $[\Gamma\phi](\mathbf{k}) = \gamma(\mathbf{k})\phi(\mathbf{k})$, $\mathbf{k} \in \mathbb{Z}^d$. Here $\ell^2(\mathbb{Z}^d)$ is set of square summable functions on the lattice \mathbb{Z}^d . Define the Hilbert space $H_\Gamma := \text{Im}(\Gamma)$. Let $X = (\mathbf{x}_1, \dots, \mathbf{x}_n)^\top \in \mathbb{T}^{n \times d}$, $Y = (y_1, \dots, y_n)^\top \in \mathbb{R}^n$ and $\mathcal{P} : H_\Gamma \rightarrow \mathbb{R}^n$ be a surjective operator such as

$$P : \phi \mapsto \left(\sum_{\mathbf{k} \in \mathbb{Z}^d} \phi(\mathbf{k}) e^{2\pi i \mathbf{x}_1^\top \mathbf{k}}, \dots, \sum_{\mathbf{k} \in \mathbb{Z}^d} \phi(\mathbf{k}) e^{2\pi i \mathbf{x}_n^\top \mathbf{k}} \right)^\top. \quad (58)$$

Then the following two problems are equivalent in the sense that $\phi_\infty = \phi_{\min}$.

(D1) The initial value problem

$$\begin{cases} \frac{d\phi(\mathbf{k})}{dt} = (\gamma(\mathbf{k}))^2 \sum_{i=1}^n \left(y_i e^{-2\pi i \mathbf{x}_i^\top \mathbf{k}} - \left[\phi * e^{-2\pi i \mathbf{x}_i^\top (\cdot)} \right](\mathbf{k}) \right) \\ \phi(\mathbf{0}) = \phi_{\text{ini}}. \end{cases}$$

(D2) The minimization problem

$$\begin{aligned} \min_{\phi - \phi_{\text{ini}} \in H_\Gamma} \sum_{\mathbf{k} \in \mathbb{Z}^d} (\gamma(\mathbf{k}))^{-2} |\phi(\mathbf{k}) - \phi_{\text{ini}}(\mathbf{k})|^2, \\ \text{s.t. } h(\mathbf{x}_i) = y_i, \quad i = 1, \dots, n. \end{aligned}$$

Proof Let $H_1 = \ell^2(\mathbb{Z}^d)$, $H_2 = \mathbb{R}^n$, and $g = \mathbf{Y}$. By definition, Γ is injective. Then by Corollary 4, we have that $\Gamma^{-1} : H_\Gamma \rightarrow \ell^2(\mathbb{Z}^d)$ exists and H_Γ is a Hilbert space with norm $\|\phi\|_{H_\Gamma} := \|\Gamma^{-1}\phi\|_{\ell^2(\mathbb{Z}^d)}$. Moreover, $\|\phi - \phi_{\text{ini}}\|_{H_\Gamma}^2 = \sum_{\mathbf{k} \in \mathbb{Z}^d} (\gamma(\mathbf{k}))^{-2} |\phi(\mathbf{k}) - \phi_{\text{ini}}(\mathbf{k})|^2$. We note that $[P^* \mathbf{Y}](\mathbf{k}) = \sum_{i=1}^n y_i e^{-2\pi i \mathbf{x}_i^\top \mathbf{k}}$ for all $\mathbf{k} \in \mathbb{Z}^d$. Thus

$$\begin{aligned} [P^* P \phi](\mathbf{k}) &= \left[P^* \left(\sum_{\mathbf{k}' \in \mathbb{Z}^d} \phi(\mathbf{k}') e^{2\pi i \mathbf{x}_i^\top \mathbf{k}'} \right)_{i=1}^n \right](\mathbf{k}) \\ &= \sum_{i=1}^n \sum_{\mathbf{k}' \in \mathbb{Z}^d} \phi(\mathbf{k}') e^{2\pi i \mathbf{x}_i^\top \mathbf{k}'} e^{-2\pi i \mathbf{x}_i^\top \mathbf{k}} \\ &= \sum_{i=1}^n \sum_{\mathbf{k}' \in \mathbb{Z}^d} \phi(\mathbf{k}') e^{-2\pi i \mathbf{x}_i^\top (\mathbf{k} - \mathbf{k}')} \\ &= \sum_{i=1}^n \left[\phi * e^{-2\pi i \mathbf{x}_i^\top (\cdot)} \right](\mathbf{k}). \end{aligned}$$

The equivalence result then follows from Corollary 4. ■

5.2 Example: Explicitizing the implicit bias for two-layer ReLU NNs

As an example, by Corollary 5, we derive the following constrained optimization problem explicitly minimizing an FP-norm (see next section), whose solution is the same as the long-time limit solution of the simplified LFP model (54), that is,

$$\min_{h - h_{\text{ini}} \in F_\gamma} \int_{\mathbb{R}^d} \left(\mathbb{E}_{a,r} \left[\frac{r^3}{16\pi^4 \|\boldsymbol{\xi}\|^{d+3}} + \frac{a^2 r}{4\pi^2 \|\boldsymbol{\xi}\|^{d+1}} \right] \right)^{-1} |\mathcal{F}[h](\boldsymbol{\xi}) - \mathcal{F}[h_{\text{ini}}](\boldsymbol{\xi})|^2 d\boldsymbol{\xi}, \quad (59)$$

subject to constraints $h(\mathbf{x}_i) = y_i$ for $i = 1, \dots, n$. The F_γ is defined in the next section. This explicit penalty indicates that the learning of DNN is biased towards functions with more power at low frequencies, which is speculated in previous works (Xu et al., 2019a; Rahaman et al., 2019; Xu et al., 2019b). For 1-d problems ($d = 1$), when $1/\xi^2$ term dominates, the

corresponding minimization problem indicates a linear spline interpolation. Similarly, when $1/\xi^4$ dominates, the minimization problem indicates a cubic spline. In general, both two power law decays together lead to a specific mixture of linear and cubic splines. For high dimensional problems, the minimization problem is difficult to be interpreted by a specific interpolation because the order of differentiation depends on d and can be fractal.

6. FP-norm and an *a priori* generalization error bound

The equivalent explicit optimization problem (59) provides a way to analyze the generalization of sufficiently wide two-layer NNs. We consider the Fourier domain with discretized frequencies. Then, we begin with the definition of an FP-norm, which naturally induces a FP-space containing all possible solutions of a target NN, whose Rademacher complexity can be controlled by the FP-norm of the target function. Thus we obtain an *a priori* estimate of the generalization error of NN by the theory of Rademacher complexity. Our *a priori* estimates follows the Monte Carlo error rates with respect to the sample size. Importantly, Our estimate unravels how frequency components of the target function affect the generalization performance of DNNs.

6.1 Problem Setup

We focus on regression problem. Assume the target function $f : \Omega := [0, 1]^d \rightarrow \mathbb{R}$. Let the training set be $S = \{(\mathbf{x}_i, y_i)\}_{i=1}^n$, where \mathbf{x}_i 's are independently sampled from an underlying distribution $\mathcal{D}(\mathbf{x})$ and $y_i = f(\mathbf{x}_i)$. We consider the square loss

$$\ell(h, \mathbf{x}, y) = |h(\mathbf{x}) - y|^2, \quad (60)$$

with population risk

$$R_{\mathcal{D}}(h) = \mathbb{E}_{\mathbf{x} \sim \mathcal{D}} \ell(h, \mathbf{x}, f(\mathbf{x})) \quad (61)$$

and empirical risk

$$R_S(h) = \frac{1}{n} \sum_{i=1}^n \ell(h, \mathbf{x}_i, y_i). \quad (62)$$

6.2 FP-space

The quantity in the minimization problem motives a definition of FP-norm, which would lead to the definition of the function space where the solution of the minimization problem lies in. We denote $\mathbb{Z}^{d*} := \mathbb{Z}^d \setminus \{\mathbf{0}\}$. Given a frequency weight function $\gamma : \mathbb{Z}^d \rightarrow \mathbb{R}^+$ or $\gamma : \mathbb{Z}^{d*} \rightarrow \mathbb{R}^+$ satisfying

$$\|\gamma\|_{\ell^2} = \left(\sum_{\mathbf{k} \in \mathbb{Z}^d} (\gamma(\mathbf{k}))^2 \right)^{\frac{1}{2}} < +\infty \quad \text{or} \quad \|\gamma\|_{\ell^2} = \left(\sum_{\mathbf{k} \in \mathbb{Z}^{d*}} (\gamma(\mathbf{k}))^2 \right)^{\frac{1}{2}} < +\infty, \quad (63)$$

we define the FP-norm for all function $h \in L^2(\Omega)$:

$$\|h\|_{\gamma} := \|\mathcal{F}[h]\|_{H_{\Gamma}} = \left(\sum_{\mathbf{k} \in \mathbb{Z}^d} (\gamma(\mathbf{k}))^{-2} |\mathcal{F}[h](\mathbf{k})|^2 \right)^{\frac{1}{2}}. \quad (64)$$

If $\gamma : \mathbb{Z}^{d^*} \rightarrow \mathbb{R}^+$ is not defined at $\boldsymbol{\xi} = \mathbf{0}$, we set $(\gamma(\mathbf{0}))^{-1} := 0$ in the above definition and $\|\cdot\|_\gamma$ is only a semi-norm of h .

Then we define the FP-space

$$\mathcal{F}_\gamma(\Omega) = \{h \in L^2(\Omega) : \|h\|_\gamma < \infty\}. \quad (65)$$

Clearly, for any γ , the FP-space is a subspace of $L^2(\Omega)$. In addition, if $\gamma : \mathbf{k} \mapsto \|\mathbf{k}\|^{-r}$ for $\mathbf{k} \in \mathbb{Z}^{d^*}$, then functions in the FP-space with $\mathcal{F}[h](\mathbf{0}) = \int_\Omega h(\mathbf{x}) \, d\mathbf{x} = 0$ form the Sobolev space $H^r(\Omega)$. Note that in the case of DNN, according to the F-Principle, $(\gamma(\mathbf{k}))^{-2}$ increases with the frequency. Thus, the contribution of high frequency to the FP-norm is more significant than that of low frequency.

6.3 a priori generalization error bound

Next, we would show the upper bound of the FP-norm of a function leads to a upper bound of the Rademacher complexity of the function space. The Rademacher complexity is defined as

$$\text{Rad}_S(\mathcal{H}) = \frac{1}{n} \mathbb{E}_\tau \left[\sup_{h \in \mathcal{H}} \sum_{i=1}^n \tau_i h(\mathbf{x}_i) \right]. \quad (66)$$

for the function space \mathcal{H} and data-set $S = \{\mathbf{x}_i, h(\mathbf{x}_i)\}_{i=1}^n$.

Lemma 5. (i) For $\mathcal{H}_Q = \{h : \|h\|_\gamma \leq Q\}$ with $\gamma : \mathbb{Z}^d \rightarrow \mathbb{R}^+$, we have

$$\text{Rad}_S(\mathcal{H}_Q) \leq \frac{1}{\sqrt{n}} Q \|\gamma\|_{\ell^2}. \quad (67)$$

(ii) For $\mathcal{H}'_Q = \{h : \|h\|_\gamma \leq Q, |\mathcal{F}[h](\mathbf{0})| \leq c_0\}$ with $\gamma : \mathbb{Z}^{d^*} \rightarrow \mathbb{R}^+$ and $\gamma^{-1}(\mathbf{0}) := 0$, we have

$$\text{Rad}_S(\mathcal{H}'_Q) \leq \frac{c_0}{\sqrt{n}} + \frac{1}{\sqrt{n}} Q \|\gamma\|_{\ell^2}. \quad (68)$$

Proof We first prove (ii) since it is more involved. By the definition of the Rademacher complexity

$$\text{Rad}_S(\mathcal{H}'_Q) = \frac{1}{n} \mathbb{E}_\tau \left[\sup_{h \in \mathcal{H}'_Q} \sum_{i=1}^n \tau_i h(\mathbf{x}_i) \right]. \quad (69)$$

Let $\tau(\mathbf{x}) = \sum_{i=1}^n \tau_i \delta(\mathbf{x} - \mathbf{x}_i)$, where τ_i 's are i.i.d. random variables with $\mathbb{P}(\tau_i = 1) = \mathbb{P}(\tau_i = -1) = \frac{1}{2}$. We have $\mathcal{F}[\tau](\mathbf{k}) = \int_\Omega \sum_{i=1}^n \tau_i \delta(\mathbf{x} - \mathbf{x}_i) e^{-2\pi i \mathbf{k}^\top \mathbf{x}} \, d\mathbf{x} = \sum_{i=1}^n \tau_i e^{-2\pi i \mathbf{k}^\top \mathbf{x}_i}$. Note that

$$\sup_{h \in \mathcal{H}'_Q} \sum_{i=1}^n \tau_i h(\mathbf{x}_i) = \sup_{h \in \mathcal{H}'_Q} \sum_{i=1}^n \tau_i \bar{h}(\mathbf{x}_i) = \sup_{h \in \mathcal{H}'_Q} \sum_{i=1}^n \tau_i \sum_{\mathbf{k} \in \mathbb{Z}^d} \overline{\mathcal{F}[h](\mathbf{k})} e^{-2\pi i \mathbf{k}^\top \mathbf{x}_i} \quad (70)$$

$$= \sup_{h \in \mathcal{H}'_Q} \sum_{\mathbf{k} \in \mathbb{Z}^d} \mathcal{F}[\tau](\mathbf{k}) \overline{\mathcal{F}[h](\mathbf{k})}. \quad (71)$$

By the Cauchy–Schwarz inequality,

$$\begin{aligned} & \sup_{h \in \mathcal{H}'_Q} \sum_{\mathbf{k} \in \mathbb{Z}^d} \mathcal{F}[\tau](\mathbf{k}) \overline{\mathcal{F}[h](\mathbf{k})} \\ & \leq \sup_{h \in \mathcal{H}_Q} \left[\mathcal{F}[\tau](\mathbf{0}) \overline{\mathcal{F}[h](\mathbf{0})} + \left(\sum_{\mathbf{k} \in \mathbb{Z}^{d^*}} (\gamma(\mathbf{k}))^2 |\mathcal{F}[\tau](\mathbf{k})|^2 \right)^{1/2} \left(\sum_{\mathbf{k} \in \mathbb{Z}^{d^*}} (\gamma(\mathbf{k}))^{-2} |\overline{\mathcal{F}[h](\mathbf{k})}|^2 \right)^{1/2} \right] \end{aligned} \quad (72)$$

$$\leq c_0 |\mathcal{F}[\tau](\mathbf{0})| + Q \left(\sum_{\mathbf{k} \in \mathbb{Z}^{d^*}} (\gamma(\mathbf{k}))^2 |\mathcal{F}[\tau](\mathbf{k})|^2 \right)^{1/2}. \quad (73)$$

Since $\mathbb{E}_\tau |\mathcal{F}[\tau](\mathbf{0})| \leq (\mathbb{E}_\tau |\mathcal{F}[\tau](\mathbf{0})|^2)^{1/2} = \sqrt{n}$, $\mathbb{E}_\tau |\mathcal{F}[\tau](\mathbf{k})|^2 = \mathbb{E}_\tau \sum_{i,j=1}^n \tau_i \tau_j e^{-2\pi i \mathbf{k}^\top (\mathbf{x}_i - \mathbf{x}_j)} = n$, we obtain

$$\mathbb{E}_\tau \left[\sup_{h \in \mathcal{H}'_Q} \sum_{i=1}^n \tau_i h(\mathbf{x}_i) \right] \leq c_0 \sqrt{n} + Q \mathbb{E}_\tau \left(\sum_{\mathbf{k} \in \mathbb{Z}^{d^*}} (\gamma(\mathbf{k}))^2 |\mathcal{F}[\tau](\mathbf{k})|^2 \right)^{1/2} \quad (74)$$

$$\leq c_0 \sqrt{n} + Q \left(\mathbb{E}_\tau \sum_{\mathbf{k} \in \mathbb{Z}^{d^*}} (\gamma(\mathbf{k}))^2 |\mathcal{F}[\tau](\mathbf{k})|^2 \right)^{1/2} \quad (75)$$

$$= c_0 \sqrt{n} + Q \sqrt{n} \|\gamma\|_{\ell^2}. \quad (76)$$

This leads to

$$\text{Rad}_S(\mathcal{H}'_Q) \leq \frac{c_0}{\sqrt{n}} + \frac{1}{\sqrt{n}} Q \|\gamma\|_{\ell^2}. \quad (77)$$

For (ii), the proof is similar to (i). We have

$$\mathbb{E}_\tau \left[\sup_{h \in \mathcal{H}_Q} \sum_{\mathbf{k} \in \mathbb{Z}^d} \mathcal{F}[\tau](\mathbf{k}) \overline{\mathcal{F}[h](\mathbf{k})} \right] \leq Q \mathbb{E}_\tau \left(\sum_{\mathbf{k} \in \mathbb{Z}^d} (\gamma(\mathbf{k}))^2 |\mathcal{F}[\tau](\mathbf{k})|^2 \right)^{1/2} \leq Q \sqrt{n} \|\gamma\|_{\ell^2}. \quad (78)$$

Therefore

$$\text{Rad}_S(\mathcal{H}_Q) \leq \frac{1}{\sqrt{n}} Q \|\gamma\|_{\ell^2}. \quad (79)$$

■

Then, we prove that the target function can be used to bound the FP-norm of the solution of the minimization problem.

Lemma 6. *Suppose that the real-valued target function $f \in \mathcal{F}_\gamma(\Omega)$ and that the training dataset $\{(\mathbf{x}_i, y_i)\}_{i=1}^n$ satisfies $y_i = f(\mathbf{x}_i)$, $i = 1, \dots, n$. If $\gamma : \mathbb{Z}^d \rightarrow \mathbb{R}^+$, then there exists a unique solution h_n to the regularized model*

$$\min_{h - h_{\text{ini}} \in \mathcal{F}_\gamma(\Omega)} \|h - h_{\text{ini}}\|_\gamma, \quad \text{s.t.} \quad h(\mathbf{x}_i) = y_i, \quad i = 1, \dots, n. \quad (80)$$

Moreover, we have

$$\|h_n - h_{\text{ini}}\|_\gamma \leq \|f - h_{\text{ini}}\|_\gamma. \quad (81)$$

Proof By the definition of the FP-norm, we have $\|h_n - h_{\text{ini}}\|_\gamma = \|\mathcal{F}[h]_n - \mathcal{F}[h]_{\text{ini}}\|_{H_\Gamma}$. According to Corollary 6, the minimizer of problem (80) exists, i.e., h_n exists. Since the target function $f(x)$ satisfies the constraints $f(x_i) = y_i$, $i = 1, \dots, n$, we have $\|h_n - h_{\text{ini}}\|_\gamma \leq \|f - h_{\text{ini}}\|_\gamma$. \blacksquare

Lemma 7. *Suppose that the real-valued target function $f \in \mathcal{F}_\gamma(\Omega)$ and the training dataset $\{(\mathbf{x}_i, y_i)\}_{i=1}^n$ satisfies $y_i = f(\mathbf{x}_i)$, $i = 1, \dots, n$. If $\gamma : \mathbb{Z}^{d^*} \rightarrow \mathbb{R}^+$ with $\gamma^{-1}(\mathbf{0}) := 0$, then there exists a solution h_n to the regularized model*

$$\min_{h - h_{\text{ini}} \in \mathcal{F}_\gamma(\Omega)} \|h - h_{\text{ini}}\|_\gamma, \quad \text{s.t.} \quad h(\mathbf{x}_i) = y_i, \quad i = 1, \dots, n. \quad (82)$$

Moreover, we have

$$|\mathcal{F}[h_n - h_{\text{ini}}](\mathbf{0})| \leq \|f - h_{\text{ini}}\|_\infty + \|f - h_{\text{ini}}\|_\gamma \|\gamma\|_{\ell^2}. \quad (83)$$

Proof Let $f' = f - h_{\text{ini}}$. Since $h_n(\mathbf{x}_i) - f(\mathbf{x}_i) = 0$ for $i = 1, \dots, n$, we have $h_n(\mathbf{x}_i) - f'(\mathbf{x}_i) - h_{\text{ini}}(\mathbf{x}_i) = 0$. Therefore

$$|\mathcal{F}[h_n - h_{\text{ini}}](\mathbf{0})| = \left| f'(\mathbf{x}_i) - \sum_{\mathbf{k} \in \mathbb{Z}^{d^*}} \mathcal{F}[h_n - h_{\text{ini}}](\mathbf{k}) e^{2\pi i \mathbf{k}^\top \mathbf{x}_i} \right| \quad (84)$$

$$\leq \|f'\|_\infty + \sum_{\mathbf{k} \in \mathbb{Z}^{d^*}} |\mathcal{F}[h_n - h_{\text{ini}}](\mathbf{k})| \quad (85)$$

$$\leq \|f'\|_\infty + \left(\sum_{\mathbf{k} \in \mathbb{Z}^{d^*}} (\gamma(\mathbf{k}))^2 \right)^{\frac{1}{2}} \left(\sum_{\mathbf{k} \in \mathbb{Z}^{d^*}} (\gamma(\mathbf{k}))^{-2} |\mathcal{F}[h_n - h_{\text{ini}}](\mathbf{k})|^2 \right)^{\frac{1}{2}} \quad (86)$$

$$\leq \|f'\|_\infty + \|h_n - h_{\text{ini}}\|_\gamma \|\gamma\|_{\ell^2} \quad (87)$$

$$\leq \|f'\|_\infty + \|f'\|_\gamma \|\gamma\|_{\ell^2}. \quad (88)$$

We remark that the last step is due to the same reason as Lemma 6. \blacksquare

Based on above analysis, we derive an *a priori* generalization error bound of the minimization problem.

Theorem 3 (*a priori* generalization error bound). *Suppose that the real-valued target function $f \in \mathcal{F}_\gamma(\Omega)$, the training dataset $\{(\mathbf{x}_i, y_i)\}_{i=1}^n$ satisfies $y_i = f(\mathbf{x}_i)$, $i = 1, \dots, n$, and h_n is the solution of the regularized model*

$$\min_{h - h_{\text{ini}} \in \mathcal{F}_\gamma(\Omega)} \|h - h_{\text{ini}}\|_\gamma, \quad \text{s.t.} \quad h(\mathbf{x}_i) = y_i, \quad i = 1, \dots, n. \quad (89)$$

Then we have

(i) given $\gamma : \mathbb{Z}^d \rightarrow \mathbb{R}^+$, for any $\delta \in (0, 1)$, with probability at least $1 - \delta$ over the random training sample, the population risk has the bound

$$R_{\mathcal{D}}(h_n) \leq \|f - h_{\text{ini}}\|_{\gamma} \|\gamma\|_{\ell^2} \left(\frac{2}{\sqrt{n}} + 4\sqrt{\frac{2 \log(4/\delta)}{n}} \right). \quad (90)$$

(ii) given $\gamma : \mathbb{Z}^{d^*} \rightarrow \mathbb{R}^+$ with $\gamma(\mathbf{0})^{-1} := 0$, for any $\delta \in (0, 1)$, with probability at least $1 - \delta$ over the random training sample, the population risk has the bound

$$R_{\mathcal{D}}(h_n) \leq (\|f - h_{\text{ini}}\|_{\infty} + 2\|f - h_{\text{ini}}\|_{\gamma} \|\gamma\|_{\ell^2}) \left(\frac{2}{\sqrt{n}} + 4\sqrt{\frac{2 \log(4/\delta)}{n}} \right). \quad (91)$$

Proof Let $f' = f - h_{\text{ini}}$ and $Q = \|f'\|_{\gamma}$.

(i) Given $\gamma : \mathbb{Z}^d \rightarrow \mathbb{R}^+$, we set $\mathcal{H}_Q = \{h : \|h - h_{\text{ini}}\|_{\gamma} \leq Q\}$. According to Lemma 6, the solution of problem (89) $h_n \in \mathcal{H}_Q$. By the relation between generalization gap and Rademacher complexity (Bartlett and Mendelson, 2002; Shalev-Shwartz and Ben-David, 2014),

$$|R_{\mathcal{D}}(h_n) - L_S(h_n)| \leq 2\text{Rad}_S(\mathcal{H}_Q) + 2 \sup_{h, h' \in \mathcal{H}_Q} \|h - h'\|_{\infty} \sqrt{\frac{2 \log(4/\delta)}{n}}. \quad (92)$$

One of the component can be bounded as follows

$$\sup_{h, h' \in \mathcal{H}_Q} \|h - h'\|_{\infty} \leq \sup_{h \in \mathcal{H}_Q} 2\|h - h_{\text{ini}}\|_{\infty} \quad (93)$$

$$\leq \sup_{h \in \mathcal{H}_Q} 2 \max_{\mathbf{x}} \left| \sum_{\mathbf{k} \in \mathbb{Z}^d} \mathcal{F}[h - h_{\text{ini}}](\mathbf{k}) e^{2\pi i \mathbf{k}^T \mathbf{x}} \right| \quad (94)$$

$$\leq \sup_{h \in \mathcal{H}_Q} 2 \sum_{\mathbf{k} \in \mathbb{Z}^d} |\mathcal{F}[h - h_{\text{ini}}](\mathbf{k})| \quad (95)$$

$$\leq 2 \sup_{h \in \mathcal{H}_Q} \left(\sum_{\mathbf{k} \in \mathbb{Z}^d} (\gamma(\mathbf{k}))^2 \right)^{\frac{1}{2}} \left(\sum_{\mathbf{k} \in \mathbb{Z}^d} (\gamma(\mathbf{k}))^{-2} |\mathcal{F}[h - h_{\text{ini}}](\mathbf{k})|^2 \right)^{\frac{1}{2}} \quad (96)$$

$$\leq 2Q \|\gamma\|_{\ell^2}. \quad (97)$$

By Lemma 5,

$$\text{Rad}_S(\mathcal{H}_Q) \leq \frac{1}{\sqrt{n}} Q \|\gamma\|_{\ell^2}. \quad (98)$$

By optimization problem (89), $L_S(h_n) \leq L_S(f') = 0$. Therefore we obtain

$$R_{\mathcal{D}}(h) \leq \frac{2}{\sqrt{n}} \|f'\|_{\gamma} \|\gamma\|_{\ell^2} + 4\|f'\|_{\gamma} \|\gamma\|_{\ell^2} \sqrt{\frac{2 \log(4/\delta)}{n}}. \quad (99)$$

(ii) Given $\gamma : \mathbb{Z}^{d^*} \rightarrow \mathbb{R}^+$ with $\gamma(\mathbf{0})^{-1} := 0$, set $c_0 = \|f'\|_{\infty} + \|f'\|_{\gamma} \|\gamma\|_{\ell^2}$. By Lemma 5, 6, and 7, define $\mathcal{H}'_Q = \{h : \|h - h_{\text{ini}}\|_{\gamma} \leq Q, |\mathcal{F}[h - h_{\text{ini}}](\mathbf{0})| \leq c_0\}$, we obtain

$$\text{Rad}_S(\mathcal{H}'_Q) \leq \frac{1}{\sqrt{n}} \|f'\|_{\infty} + \frac{2}{\sqrt{n}} \|f'\|_{\gamma} \|\gamma\|_{\ell^2}. \quad (100)$$

Also

$$\sup_{h, h' \in \mathcal{H}'_Q} \|h - h'\|_\infty \leq \sup_{h \in \mathcal{H}'_Q} 2 \sum_{\mathbf{k} \in \mathbb{Z}^d} |\mathcal{F}[h - h_{\text{ini}}](\mathbf{k})| \quad (101)$$

$$\leq 2 \sup_{h \in \mathcal{H}'_Q} \left[|\mathcal{F}[h - h_{\text{ini}}](\mathbf{0})| + \left(\sum_{\mathbf{k} \in \mathbb{Z}^{d*}} (\gamma(\mathbf{k}))^2 \right)^{\frac{1}{2}} \left(\sum_{\mathbf{k} \in \mathbb{Z}^{d*}} (\gamma(\mathbf{k}))^{-2} |\mathcal{F}[h - h_{\text{ini}}](\mathbf{k})|^2 \right)^{\frac{1}{2}} \right] \quad (102)$$

$$\leq 2\|f'\|_\infty + 4\|f'\|_\gamma \|\gamma\|_{\ell^2}. \quad (103)$$

Then

$$R_{\mathcal{D}}(h_n) \leq \frac{2}{\sqrt{n}} \|f'\|_\infty + \frac{4}{\sqrt{n}} \|f'\|_\gamma \|\gamma\|_{\ell^2} + (4\|f'\|_\infty + 8\|f'\|_\gamma \|\gamma\|_{\ell^2}) \sqrt{\frac{2 \log(4/\delta)}{n}}. \quad (104)$$

■

Remark 5. *By the assumption in the theorem, the target function f belongs to $\mathcal{F}_\gamma(\Omega)$ which is a subspace of $L^2(\Omega)$. In most applications, f is also a continuous function. In any case, f can be well-approximated by a large neural network due to universal approximation theory (Cybenko, 1989).*

Our a priori generalization error bound in Theorem 3 is large if the target function possesses significant high frequency components. Thus, it explains the failure of DNNs in generalization for learning the parity function (Shalev-Shwartz et al., 2017), whose power concentrates at high frequencies. In the following, We use experiments to illustrate that, as predicted by our a priori generalization error bound, larger FP-norm of the target function indicates a larger generalization error.

7. Numerical experiments

In this section, we conduct numerical experiments to validate the effectiveness of LFP model for two-layer ReLU and Tanh networks. In addition, we would show that, with sufficient samples, the test error still increases as the frequency of the target function increases. The procedure to numerically solve the LFP model can be found in Appendix B[†].

7.1 The effectiveness of LFP model

Without the last term in Eq. (35) arising from the evolution of \mathbf{w} , we would show that the simplified LFP model in 54 can still predict the learning results of two-layer wide NNs.

For 1d input example of ReLU NN, when the term of $1/\xi^4$ dominates, as shown in Fig. 2(a), the NN interpolates training data by a smooth function (denoted by f_{NN} , red solid), which nearly overlaps with the prediction of LFP model (denoted by f_{LFP} and the cubic spline interpolation (grey dashed). On the contrary, when the term of $1/\xi^2$ dominates, as

[†]. The code can be found at <https://github.com/xuzhiqin1990/LFP>

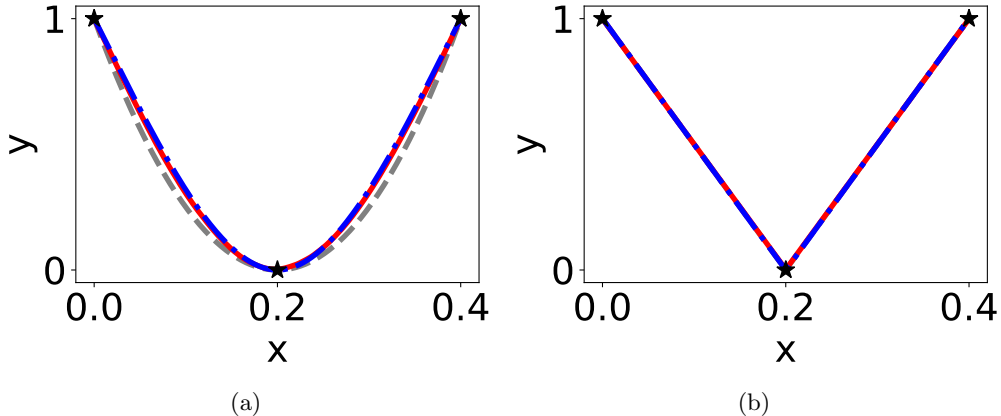


Figure 2: f_{NN} (red solid) vs. f_{LFP} (blue dashed dot) vs. splines (grey dashed, cubic spline for (a) and linear spline for (b)) for a 1-d problem. All curves nearly overlap with one other. Two-layer ReLU NN of 10000 hidden neurons is initialized with (a) $\langle r^2 \rangle_r \gg \langle a^2 \rangle_a$, and (b) $\langle r^2 \rangle_r \ll \langle a^2 \rangle_a$. Black stars indicates training data.

shown in Fig. 2(b), the NN interpolates training data by a function, which nearly overlaps with the prediction of LFP model and the linear spline interpolation. These result are consistent with above analysis.

For 2d input example of ReLU NN, we consider the XOR problem, which cannot be solved by one-layer neural networks (Minsky and Papert, 2017). The training samples consist of four points represented by black stars in Fig. 3(a). As shown in Fig. 3(b), our LFP model predicts accurately outputs of the well-trained NN over the input domain $[-1, 1]^2$.

For two-layer Tanh NN, the weight coefficient decays exponentially w.r.t. the frequency no matter which part dominates, thus, the NN always learns the training data by a smooth function, as shown in Fig. 4.

7.2 Generalization error

In this section, we train a ReLU-NN of width 1-5000-1 to fit 20 uniform samples of $f(x) = \sin(2\pi vx)$ on $[0, 1]$ until the training MSE loss is smaller than 10^{-6} , where v is the frequency. The number of training sample is sufficient to recover the frequency of the target function by the Nyquist sampling theorem. We then use 500 uniform samples to test the NN. As the frequency of the target function increases, the FP-norm would increase, thus, leading to a looser bound of the generalization error. As shown in Fig. 5, the test error increases as the frequency of the target function increases.

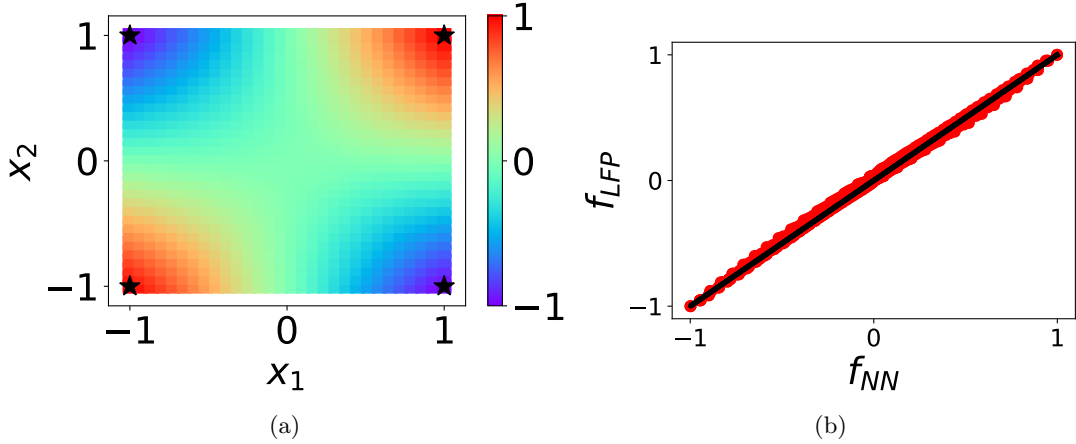


Figure 3: 2-d XOR problem with four training data indicated by black stars learned by a two-layer ReLU NN of 80000 hidden neurons. (a) f_{NN} illustrated in color scale. (b) f_{LFP} (ordinate) vs. f_{NN} (abscissa) represented by red dots evaluated over whole input domain $[-1, 1]^2$. The black line indicates the identity function.

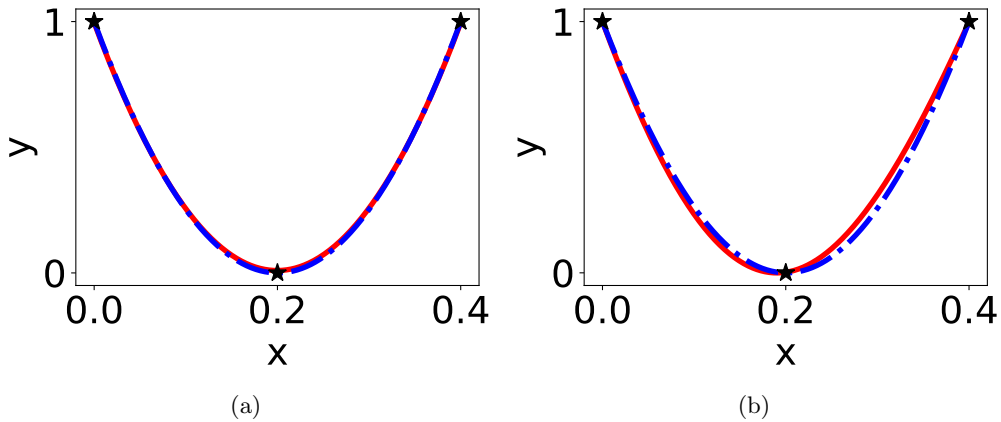


Figure 4: f_{NN} (red solid) vs. f_{LFP} (blue dashed dot) for a 1-d problem. Two-layer tanh NN of 10000 hidden neurons is initialized with (a) $\langle r^2 \rangle_r \gg \langle a^2 \rangle_a$, and (b) $\langle r^2 \rangle_r \ll \langle a^2 \rangle_a$. Black stars indicates training data.

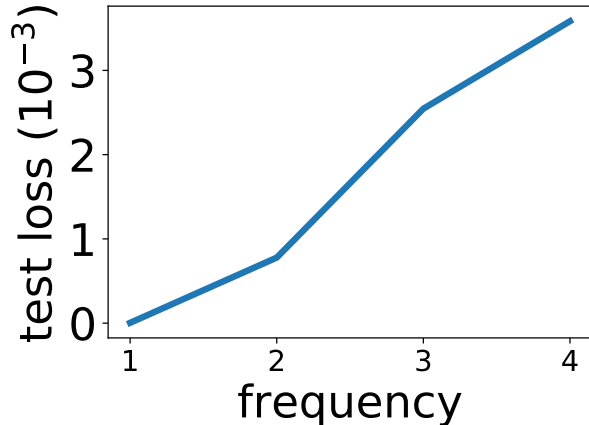


Figure 5: Test loss are plotted as a function of frequency v of the target function $\sin(2\pi vx)$.

8. Discussion

In this work, inspired by the F-Principle, we derive an LFP model for two layer wide NNs — a model quantitatively well predicts the output of two-layer ReLU and tanh NNs in an extremely over-parameterized regime. We explicitize the implicit bias of the F-Principle by a constrained optimization problem equivalent to the LFP model. This explicitization leads to an *a priori* estimate of the generalization error bound, which depends on the FP-norm of the target function. Note that, our LFP model for other transfer functions can also be derived similarly.

The LFP model advances our qualitative/empirical understandings of the F-Principle to a quantitative level. i) With ASI trick (Zhang et al., 2020) offsetting the initial DNN output to zero, the LFP model indicates that the F-Principle also holds for DNNs initialized with large weights. Therefore, “initialized with small parameters” (Xu et al., 2019a,b) is not a necessary condition for the F-Principle. ii) Based on the training behavior of F-Principle, previous works (Xu et al., 2019a,b; Rahaman et al., 2019) speculate that “DNNs prefer to learn the training data by a low frequency function”. With an equivalent optimization problem explicitizing the F-Principle, this speculation is demonstrated theoretically by the LFP model.

Our *a priori* generalization error bound increases as the FP-norm of the target function increases. This explains several important phenomena. First, DNNs fail to generalize well for the parity function (Shalev-Shwartz et al., 2017). Xu et al. (2019b) shows that this is due to the inconsistency between the high frequency dominant property of the parity function and the low frequency preference of DNNs. In this work, by our *a priori* generalization error bound, the dominant high frequency of the parity function quantitatively results in a large FP-norm, thus, a large generalization error. Second, because randomly labeled data possesses large high frequency components, which induces a large FP-norm of any function well matches the training data and test data, we expect a very large generalization error, e.g., no generalization, as observed in experiments. Intuitively, our estimate indicates good generalization of NNs for well-structured low-frequency dominant real dataset as well as

bad generalization of NNs for randomly labeled data, thus providing insight into the well known puzzle of generalization of DNNs (Zhang et al., 2017).

The F-Principle, a widely observed implicit bias of DNNs, is also a natural bias for human. Empirically, when a human see several points of training data, without a specific prior, one tends to interpolate these points by a low frequency dominant function. Therefore, the success of DNN may partly result from its adoption of a similar interpolation bias as human's. In general, there could be multiple types of implicit biases underlying the training dynamics of a DNN. Inspired by the LFP model, discovering and explicitizing these implicit biases could be a key step towards a thorough quantitative understanding of deep learning.

Appendix A. Fourier transform table

We list some useful and well-known results for one-dimensional Fourier transform in Table 1. We also list some useful and well-known results for high-dimensional Fourier transform

Function of x	Fourier transform with respect to x
$g(ax)$	$\frac{1}{ a }\mathcal{F}[g]\left(\frac{\xi}{a}\right)$
$g(x - c)$	$\mathcal{F}[g](\xi)e^{-2\pi ic\xi}$
$x^k g(x)$	$\left(\frac{i}{2\pi}\right)^k \frac{d^k}{d\xi^k} \mathcal{F}[g](\xi)$
$g^{(k)}(x)$	$(2\pi i\xi)^k \mathcal{F}[g](\xi)$
1	$\delta(\xi)$
x^k	$\left(\frac{i}{2\pi}\right)^k \delta^{(k)}(\xi)$
$\delta(x - x_0)$	$e^{-2\pi i x_0 \xi}$
$H(x)$ (Heaviside)	$\frac{1}{i2\pi\xi} + \frac{1}{2}\delta(\xi)$
ReLU(x)	$-\frac{1}{4\pi^2\xi^2} + \frac{i}{4\pi}\delta'(\xi)$
$\tanh(x)$	$-i\pi\text{csch}(\pi^2\xi)$
Sigmoid(x)	$-i\pi\text{csch}(2\pi^2\xi) + \frac{1}{2}\delta(\xi)$
$\text{sech}^2(x)$	$2\pi^2\xi\text{csch}(\pi^2\xi)$
$x\text{sech}^2(x)$	$i\pi(1 - \pi^2\xi\coth(\pi^2\xi))\text{csch}(\pi^2\xi)$

Table 1: Fourier transform for 1-dimensional functions.

in Table 2.

Function of \mathbf{x}	Fourier transform with respect to \mathbf{x}
$g(a\mathbf{x})$	$\frac{1}{ a ^d} \mathcal{F}[g]\left(\frac{\boldsymbol{\xi}}{a}\right)$
$\delta(\mathbf{x} - \mathbf{x}_0)$	$e^{-2\pi i \boldsymbol{\xi}^\top \mathbf{x}_0}$
$g(\boldsymbol{\nu}^\top \mathbf{x})$ (unit vector $\boldsymbol{\nu}$)	$\delta_{\boldsymbol{\nu}}(\boldsymbol{\xi}) \mathcal{F}[g](\boldsymbol{\xi}^\top \boldsymbol{\nu})$
$g(\mathbf{w}^\top \mathbf{x} + b)$	$\delta_{\mathbf{w}}(\boldsymbol{\xi}) \mathcal{F}[g]\left(\frac{\boldsymbol{\xi}^\top \hat{\mathbf{w}}}{\ \mathbf{w}\ }\right) e^{2\pi i \frac{b}{\ \mathbf{w}\ } \boldsymbol{\xi}^\top \hat{\mathbf{w}}}$
$g(\mathbf{w}^\top \mathbf{x} + \ \mathbf{w}\ c)$	$\delta_{\mathbf{w}}(\boldsymbol{\xi}) \mathcal{F}[g]\left(\frac{\boldsymbol{\xi}^\top \hat{\mathbf{w}}}{\ \mathbf{w}\ }\right) e^{2\pi i c \boldsymbol{\xi}^\top \hat{\mathbf{w}}}$
$\mathbf{x}g(\mathbf{x})$	$\frac{i}{2\pi} \nabla \mathcal{F}[g](\boldsymbol{\xi})$
$\mathbf{x}^\perp g(\mathbf{w}^\top \mathbf{x} + \ \mathbf{w}\ c)$	$\frac{i}{2\pi} \nabla_{\boldsymbol{\xi}^\perp} \left[\delta_{\mathbf{w}}(\boldsymbol{\xi}) \mathcal{F}[g]\left(\frac{\boldsymbol{\xi}^\top \hat{\mathbf{w}}}{\ \mathbf{w}\ }\right) e^{2\pi i c \boldsymbol{\xi}^\top \hat{\mathbf{w}}} \right]$
$\mathbf{x}g(\mathbf{w}^\top \mathbf{x} + b)$	$\frac{i}{2\pi} \nabla_{\boldsymbol{\xi}} \left[\delta_{\mathbf{w}}(\boldsymbol{\xi}) \mathcal{F}[g]\left(\frac{\boldsymbol{\xi}^\top \hat{\mathbf{w}}}{\ \mathbf{w}\ }\right) e^{2\pi i b \boldsymbol{\xi}^\top \hat{\mathbf{w}} / \ \mathbf{w}\ } \right]$

Table 2: Fourier transform for d -dimensional functions

Appendix B. Numerically solve the optimization problem

Numerically, we solve the following problem

$$\min_{a_n, b_n} \sum_{i=1}^M \left(\sum_{j \in I} \left[a_j \sin\left(2\pi \frac{j}{L'} x_i\right) + b_j \cos\left(2\pi \frac{j}{L'} x_i\right) \right] - y_i \right)^2 + \epsilon \sum_{j \in I} w \left(2\pi \frac{j}{L'}\right)^{-1} (a_j^2 + b_j^2), \quad (105)$$

where we set $I = \{0, \dots, \frac{L'}{L}K - 1\}$, $L' = 10L$, L is the range of the training inputs, $K = 200$ which is much larger than the number of training samples, $\epsilon = 10^{-6}$. We can rewrite the above problem into the vector form

$$\min_{\mathbf{a}} (\mathbf{E}\mathbf{a} - \mathbf{Y})^\top (\mathbf{E}\mathbf{a} - \mathbf{Y}) + \epsilon \mathbf{a}^\top \mathbf{W}^{-1} \mathbf{a}, \quad (106)$$

where

$$\begin{aligned} \mathbf{a} &= [a_0, \dots, a_{\frac{L'}{L}K-1}, b_0, \dots, b_{\frac{L'}{L}K-1}]^\top, \\ \mathbf{E} &= [\sin(2\pi \frac{0}{L'} X), \dots, \sin(2\pi (\frac{K}{L} - 1) X), \cos(2\pi \frac{0}{L'} X), \dots, \cos(2\pi (\frac{K}{L} - 1) X)], \\ \mathbf{X} &= [x_1, \dots, x_M]^\top, \quad \mathbf{Y} = [y_1, \dots, y_M]^\top. \end{aligned}$$

The solution of the above problem satisfies

$$\mathbf{E}^\top (\mathbf{E}\mathbf{a} - \mathbf{Y}) + \epsilon \mathbf{W}^{-1} \mathbf{a} = 0. \quad (107)$$

Then \mathbf{a} is solved as

$$\mathbf{a} = [\mathbf{E}^\top \mathbf{E} + \epsilon \mathbf{W}^{-1}]^{-1} \mathbf{E}^\top \mathbf{Y}. \quad (108)$$

Acknowledgements

Z.X. is supported by National Key R&D Program of China (2019YFA0709503), and Shanghai Sailing Program. This work is also partially supported by HPC of School of Mathematical Sciences at Shanghai Jiao Tong University.

References

- A comparative analysis of the optimization and generalization property of two-layer neural network and random feature models under gradient descent dynamics. *Science China Mathematics*, pages 1–24, 2020.
- Sanjeev Arora, Simon S Du, Wei Hu, Zhiyuan Li, and Ruosong Wang. Fine-grained analysis of optimization and generalization for overparameterized two-layer neural networks. *arXiv preprint arXiv:1901.08584*, 2019.
- Devansh Arpit, Stanislaw Jastrzbski, Nicolas Ballas, David Krueger, Emmanuel Bengio, Maxinder S Kanwal, Tegan Maharaj, Asja Fischer, Aaron Courville, Yoshua Bengio, et al. A closer look at memorization in deep networks. In *Proceedings of the 34th International Conference on Machine Learning-Volume 70*, pages 233–242, 2017.
- Peter L Bartlett and Shahar Mendelson. Rademacher and gaussian complexities: Risk bounds and structural results. *Journal of Machine Learning Research*, 3(Nov):463–482, 2002.
- Ronen Basri, David Jacobs, Yoni Kasten, and Shira Kritchman. The convergence rate of neural networks for learned functions of different frequencies. In *Advances in Neural Information Processing Systems*, pages 4763–4772, 2019.
- Ronen Basri, Meirav Galun, Amnon Geifman, David Jacobs, Yoni Kasten, and Shira Kritchman. Frequency bias in neural networks for input of non-uniform density. *arXiv preprint arXiv:2003.04560*, 2020.
- Simon Biland, Vinicius C Azevedo, Byungsoo Kim, and Barbara Solenthaler. Frequency-aware reconstruction of fluid simulations with generative networks. *arXiv preprint arXiv:1912.08776*, 2019.
- Blake Bordelon, Abdulkadir Canatar, and Cengiz Pehlevan. Spectrum dependent learning curves in kernel regression and wide neural networks. *arXiv preprint arXiv:2002.02561*, 2020.
- Wei Cai, Xiaoguang Li, and Lizuo Liu. A phase shift deep neural network for high frequency approximation and wave problems. *Accepted by SISC*, *arXiv:1909.11759*, 2019.
- Yuan Cao, Zhiying Fang, Yue Wu, Ding-Xuan Zhou, and Quanquan Gu. Towards Understanding the Spectral Bias of Deep Learning. *arXiv:1912.01198 [cs, stat]*, 2019.
- George Cybenko. Approximation by superpositions of a sigmoidal function. *Mathematics of control, signals and systems*, 2(4):303–314, 1989.

- Weinan E, Chao Ma, and Lei Wu. Machine learning from a continuous viewpoint, i. *Science China Mathematics*, pages 1–34, 2020.
- Ameya D. Jagtap, Kenji Kawaguchi, and George Em Karniadakis. Adaptive activation functions accelerate convergence in deep and physics-informed neural networks. *Journal of Computational Physics*, 404:109136, 2020. doi: 10.1016/j.jcp.2019.109136.
- Ziqi Liu, Wei Cai, and Zhi-Qin John Xu. Multi-scale deep neural network (mscalednn) for solving poisson-boltzmann equation in complex domains. *Accepted by Communications in Computational Physics arXiv:2007.11207*, 2020.
- Tao Luo, Zheng Ma, Zhi-Qin John Xu, and Yaoyu Zhang. Theory of the frequency principle for general deep neural networks. *arXiv preprint arXiv:1906.09235*, 2019.
- Chao Ma, Lei Wu, and Weinan E. The slow deterioration of the generalization error of the random feature model. In *Mathematical and Scientific Machine Learning*, pages 373–389. PMLR, 2020.
- Chris Mingard, Joar Skalse, Guillermo Valle-Pérez, David Martínez-Rubio, Vladimir Mikulik, and Ard A Louis. Neural networks are a priori biased towards boolean functions with low entropy. *arXiv preprint arXiv:1909.11522*, 2019.
- Marvin Minsky and Seymour A Papert. *Perceptrons: An introduction to computational geometry*. MIT press, 2017.
- Preetum Nakkiran, Gal Kaplun, Dimitris Kalimeris, Tristan Yang, Benjamin L Edelman, Fred Zhang, and Boaz Barak. Sgd on neural networks learns functions of increasing complexity. In *Advances in Neural Information Processing Systems*, pages 3491–3501, 2019.
- Nasim Rahaman, Devansh Arpit, Aristide Baratin, Felix Draxler, Min Lin, Fred A Hamprecht, Yoshua Bengio, and Aaron Courville. On the spectral bias of deep neural networks. *International Conference on Machine Learning*, 2019.
- Shai Shalev-Shwartz and Shai Ben-David. *Understanding machine learning: From theory to algorithms*. Cambridge university press, 2014.
- Shai Shalev-Shwartz, Ohad Shamir, and Shaked Shammah. Failures of gradient-based deep learning. In *International Conference on Machine Learning*, pages 3067–3075, 2017.
- Guillermo Valle-Perez, Chico Q Camargo, and Ard A Louis. Deep learning generalizes because the parameter-function map is biased towards simple functions. *The International Conference on Learning Representations*, 2019.
- Zhi-Qin J Xu, Yaoyu Zhang, and Yanyang Xiao. Training behavior of deep neural network in frequency domain. *International Conference on Neural Information Processing*, pages 264–274, 2019a.
- Zhi-Qin John Xu, Yaoyu Zhang, Tao Luo, Yanyang Xiao, and Zheng Ma. Frequency principle: Fourier analysis sheds light on deep neural networks. *Accepted by Communications in Computational Physics, arXiv:1901.06523*, 2019b.

- Zhiqin John Xu. Understanding training and generalization in deep learning by fourier analysis. *arXiv preprint arXiv:1808.04295*, 2018.
- Greg Yang and Hadi Salman. A fine-grained spectral perspective on neural networks. *arXiv preprint arXiv:1907.10599*, 2019.
- Chiyuan Zhang, Samy Bengio, Moritz Hardt, Benjamin Recht, and Oriol Vinyals. Understanding deep learning requires rethinking generalization. *The International Conference on Learning Representations*, 2017.
- Yaoyu Zhang, Zhi-Qin John Xu, Tao Luo, and Zheng Ma. Explicitizing an implicit bias of the frequency principle in two-layer neural networks. *arXiv preprint arXiv:1905.10264*, 2019.
- Yaoyu Zhang, Zhi-Qin John Xu, Tao Luo, and Zheng Ma. A type of generalization error induced by initialization in deep neural networks. In *Mathematical and Scientific Machine Learning*, pages 144–164. PMLR, 2020.